Field Demonstrations of Chemiresistor and Surface Acoustic Wave Microchemical Sensors at the Nevada Test Site

Clifford K. Ho, Jerome Wright, Lucas K. McGrath, Eric R. Lindgren, K. Scott Rawlinson, and Charles F. Lohrstorfer

Sandia National Laboratories

Field Demonstrations of Chemiresistor and Surface Acoustic Wave Microchemical Sensors at the Nevada Test Site

Clifford K. Ho, Jerome Wright, Lucas K. McGrath, Eric R. Lindgren, K. Scott Rawlinson
Sandia National Laboratories
P.O. Box 5800
Albuquerque, New Mexico 87185-0735
Contact: ckho@sandia.gov
(505) 844-2384

Charles F. Lohrstorfer
Bechtel Nevada Corporation
P.O. Box 98521, M/S NLV082
Las Vegas, NV 89193

Abstract

Microchemical sensors developed at Sandia National Laboratories were tested at the Nevada Test Site as part of the Advanced Monitoring Systems Initiative program. Two sensors, the chemiresistor sensor and the surface-acoustic-wave (SAW) sensor, were evaluated in the tests. Both sensors rely on sorption of chemicals onto polymer films to produce a change in an electrical signal that can be recorded and calibrated, but different transduction mechanisms are used. The primary purpose of the tests was to evaluate the feasibility of using these devices in potentially long-term, unattended applications such as long-term monitoring of subsurface contaminants. A complete monitoring system was developed that provided real-time monitoring of the sensors via the internet. Engineering issues such as sensor packaging, data acquisition, power requirements, and telemetry were addressed during the development and testing of the sensor systems. In addition, issues such as data processing, noise, and interferences from fluctuating environmental variables were also encountered and evaluated during the field tests. Results showed that both sensors could be operated remotely and continuously for long-term monitoring applications using commercial data-acquisition systems and custom-designed packaging. Both the chemiresistor and SAW sensors experienced drift in the signal and were impacted by fluctuations in temperature and humidity. However, results from the chemiresistor showed that exposure to large concentrations of contaminants (e.g., trichloroethylene) overwhelmed the fluctuations caused by temperature and humidity variations. Results also showed that the chemiresistor sensor exhibited better stability and sensitivity than the SAW sensor for the conditions and analytes that were tested, which was contrary to initial theoretical predictions.

Acknowledgments

Contents

List of Figures

List of Tables

1. Introduction

1.1 Background

Nearly all of the Department of Energy (DOE) complexes, including the Closure Sites, must deal with contaminated subsurface sites containing volatile organic compounds (e.g., TCE). Plans for remediation and long-term stewardship of these sites will require monitoring. However, current methods employing manual grab samples with off-site laboratory analysis are extremely costly and time-consuming. For example, the DOE Savannah River Site requires manual collection of nearly 40,000 groundwater samples per year, which can cost between $100 to $1,000 per sample for off-site analysis (not including the cost of collection). In addition, the integrity of off-site analyses can be compromised during sample collection, transport, and storage. An attractive alternative is the use of real-time sensors that can be placed *in situ*, which would reduce the need for manual samples and expensive off-site analyses. While technologies exists to detect and analyze volatile organic compounds (VOCs), very few systems are designed to be deployed *in situ* (e.g., in soil and water) while providing real-time, continuous, long-term monitoring. Many of these existing technologies (e.g., gas chromatography, photoionization) include sensitive electronic components and require the flow of a carrier gas during operation, which may not be amenable to long-term *in-situ* monitoring applications.

1.2 Purpose

The purpose of this work is to develop simple, rugged, *in-situ* microchemical sensors and systems that can be used to provide unattended real-time monitoring and characterization of VOCs in soil and groundwater. The intent is to vastly reduce the projected baseline costs associated with monitoring DOE sites contaminated with VOCs. In addition, we hope to improve public and stakeholder confidence in our ability to carry out long-term stewardship of contaminated sites through the use of continuous *in-situ* monitoring systems. The technology for these devices can also be used in other arenas where volatile organic compounds need to be monitored continuously *in situ* (e.g., Homeland Security, process monitoring, worker safety, etc.).

The specific intent of the field tests described in this report is to identify and address "real-world" engineering issues and uncertainties that may impact the performance of the sensors. These issues include sensor packaging, emplacement methods, data acquisition, telemetry, power requirements, data processing, and dealing with interferences and uncontrolled environments in the field (e.g., diurnal fluctuations in temperature and humidity, unknown constituents, etc.). These factors are difficult to assess in controlled laboratory environments.

1.3 Overview of Report

This report first provides a brief description of the two microchemical sensors that were evaluated and tested in this study. The operation, packaging, and calibration of the chemiresistor and surface-acoustic-wave (SAW) sensors are described. A description of the field tests that were conducted at the HAZMAT Spill Center at the Nevada Test Site are then presented. A

description of the tests is provided, along with a discussion of the data acquisition methods, telemetry, and data processing. Results of the tests are presented followed by a discussion of issues that were identified. Recommendations to address these issues and improve the performance of the sensors are then presented along with a summary of the findings.

2. Description of Sensors

2.1 Chemiresistor Sensor

2.1.1 Operation

The chemiresistor sensors used in the field tests at the Nevada Test Site detect VOC vapors via conductive polymer films that are deposited onto micro-fabricated circuits. The chemically-sensitive polymer is dissolved in a solvent and mixed with conductive carbon particles. The resulting ink is then deposited and dried onto thin-film platinum traces on a solid substrate (chip). When chemical vapors come into contact with the polymers, the chemicals absorb into the polymers, causing them to swell. The swelling changes the resistance of the electrode, which can be measured and recorded using a data logger or an ohmmeter (see Figure 1). The swelling is reversible if the chemical vapors are removed, but some hysteresis can occur at high concentration exposures. The amount of swelling corresponds to the concentration of the chemical vapor in contact with the chemiresistor, so these devices can be calibrated by exposing the chemiresistors to known concentrations of target analytes.
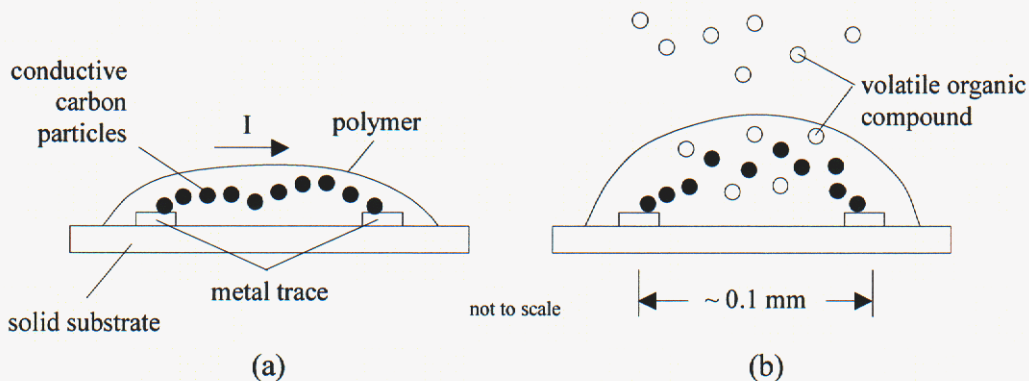
Figure 1. VOC detection by a thin-film chemiresistor: (a) Electrical current (I) flows across a conductive thin-film carbon-loaded polymer deposited on a micro-fabricated electrode; (b) VOCs absorb into the polymer, causing it to swell (reversibly) and break some of the conductive pathways, which increases the electrical resistance.

Figure 2 shows the architecture of the microsensor, which integrates an array of chemiresistors with a temperature sensor and heating elements (Hughes et al., 2000). The chemiresistor array has been shown to detect a variety of VOCs including aromatic hydrocarbons (e.g., benzene), chlorinated solvents (e.g., trichloroethylene (TCE), carbon tetrachloride), aliphatic hydrocarbons

(e.g., hexane, iso-octane), alcohols, and ketones (e.g., acetone). The on-board temperature sensor comprised of a thin-film platinum trace can be used to not only monitor the in-situ temperature, but it can also provide a means for temperature control. A feedback control system between the temperature sensor and on-board heating elements can allow the chemiresistors to be maintained at a fairly constant temperature, which can aid in the processing of data when comparing the responses to calibrated training sets. In addition, the chemiresistors can be maintained at a temperature above the ambient to prevent condensation of water, which may be detrimental to the wires and surfaces of the chemiresistor.
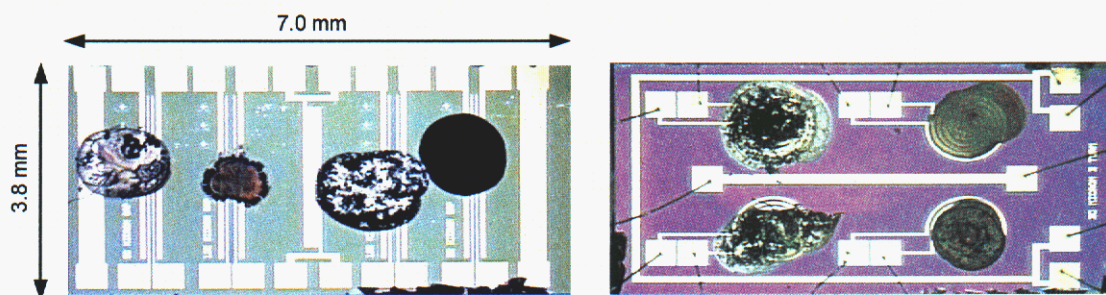
Figure 2. Chemiresistor arrays developed at Sandia with four conductive polymer films (black spots) deposited onto a microfabricated circuit. Left: Linear-electrode design (C4) with a temperature sensor in the middle and heating elements on the ends. Right: New spiral-electrode design (E2) with temperature sensor on the perimeter and heating element in the middle.

2.1.2 Packaging

A robust package has been designed and fabricated to house the chemiresistor array (Ho and Hughes, 2002). This cylindrical package is small (~ 3 cm diameter) and is constructed of rugged, chemically-resistant material. Early designs have used PEEK (PolyEtherEtherKetone), a semi-crystalline, thermoplastic with excellent resistance to chemicals and fatigue. Newer package designs have been fabricated from stainless steel (Figure 3). The package design is modular and can be easily taken apart (unscrewed like a flashlight) to replace the chemiresistor sensor if desired. Fitted with Viton O-rings, the package is completely waterproof, but gas is allowed to diffuse through a GORE-TEX® membrane that covers a small window to the sensor. Like clothing made of GORE-TEX®, the membrane prevents liquid water from passing through it, but the membrane "breathes," allowing vapors to diffuse through. Even in water, dissolved VOCs can partition across the membrane into the gas-phase headspace next to the chemiresistors to allow detection of aqueous-phase contaminants. The aqueous concentrations can be determined from the measured gas-phase concentrations using Henry's Law. Mechanical protection is also provided via a perforated metal plate that covers the chemiresistors. The chemiresistors are situated on a 16-pin dual-in-line package that is connected to a weatherproof cable, which can be of any length because of the DC-resistance measurement. The cable can be connected to a hand-held multimeter for manual single-channel readings, or it can be connected to a multi-channel data logger for long-term, remote operation.
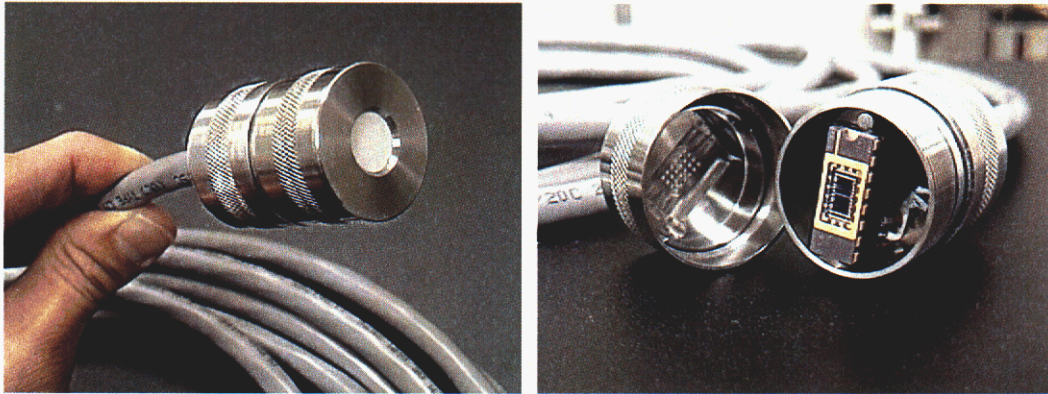
Figure 3. Stainless-steel waterproof package that houses the chemiresistor array. Left: GORE-TEX® membrane covers a small window over the chemiresistors. Right: Disassembled package exposing the 16-pin dual-in-line package and chemiresistor chip.

2.2 Surface Acoustic Wave Sensor

2.2.1 Operation

Surface-acoustic-wave (SAW) sensors consist of an input transducer, a chemically adsorbent polymer film, and an output transducer on a peizoelectric substrate, which is typically quartz (see Figure 4). The input transducer launches an acoustic wave that travels through the chemical film and is detected by the output transducer. The Sandia-made device runs at a very high frequency (approximately 525 MHz), and the velocity and attenuation of the signal are sensitive to the viscoelasticity and mass of the thin film. SAWS have been able to distinguish organophosphates, chlorinated hydrocarbons, ketones, alcohols, aromatic hydrocarbons, saturated hydrocarbons, and water.
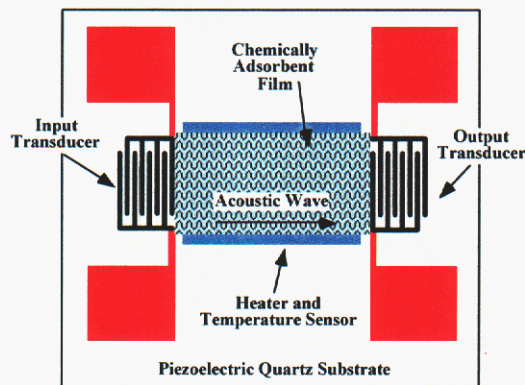
Figure 4. Schematic of SAW device.

The SAW used in these tests have four channels—each channel consisting of a transmitter and a receiver, separated by a small distance. Three of the four channels have a polymer deposited on the substrate between the transmitter and receiver (Figure 5). The purpose of the polymers is to adsorb chemicals of interest, with different polymers having different affinities to various chemicals. When a chemical is absorbed, the mass of the polymer increases, causing a slight change in phase relative to the reference (fourth) channel, which does not contain a polymer. The SAW device also contains three Application Specific Integrated Circuit chips (ASICs), which contain the electronics to analyze the signals and provide a DC voltage signal proportional to the phase shift. The SAW device, containing the transducers and ASICs, is bonded to a piece of quartz glass, which is placed in a leadless chip carrier (LCC) (see Figure 5). Wire bonds connect the terminals of the leadless chip carrier to the SAW circuits.
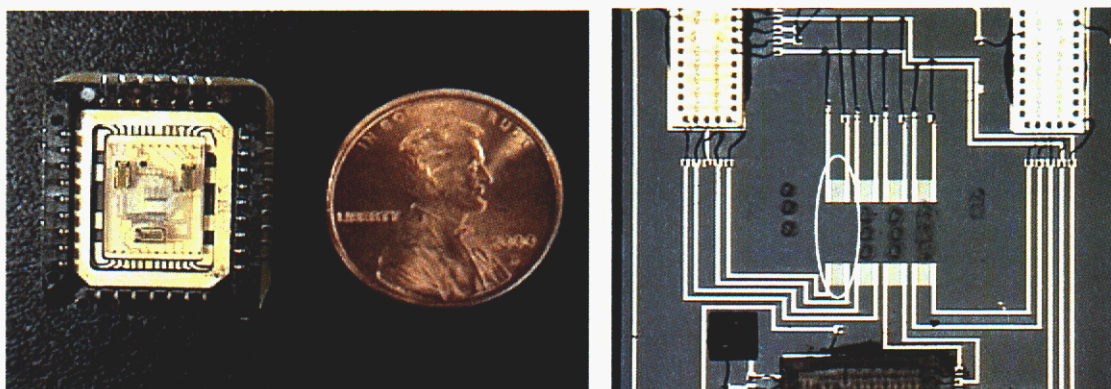
Figure 5. Left: Four-channel SAW packaged in a leadless chip carrier. Right: Close-up of four channels for SAW P9. Three of the four have polymer depositions. The fourth channel (circled) is the reference channel.

2.2.2 Packaging

A rugged package was designed for the SAW sensor to allow it to be used in subsurface environments. The design of the SAW sensor housing was modeled after the chemiresistor assembly, resulting in time ands costs savings, as well as interchangeability between the two sensor types. The primary difference between the chemiresistor housing and the SAW housing is that the outer collar for the SAW sensor is longer to accommodate additional electronics on a circuit board.

The assembly consists of a stainless steel housing, a signal-conditioning board, a SAW interface circuit board, a supporting structure for the circuits, a sensor cap, and a manifold for a future pre-concentrator. The signal-conditioning board contains a 4-channel op-amp and associated resistors (unity gain), a voltage regulator (see below), and interface connectors. The op-amp provides isolation, and therefore some level of protection, between the SAW and the measuring equipment. Since there are three outputs from the SAW device, one channel of the op-amp is not used. The SAW interface circuit board carries the traces to the SAW socket/LCC.

15

The voltage regulator was to provide the 3.3 Volts DC (VDC) required by the SAW. However, the required 3.3 VDC was not maintained with the SAW device drawing its nominal 100-110 mA. As a result, the voltage regulator was replaced with an external potted power supply. This alternative external power supply worked very well—the only required input was 12-30 VDC, and the device outputs both 3.3 VDC for the SAW power and +/- 15VDC for the op-amp power.

A support structure provides the surfaces to structurally attach the circuit boards, and it was designed to be secured by the existing 4-40 screws in the housing. Originally, this structure was made from PEEK, however it proved difficult to bond the individual parts with any rigidity. Therefore future sets were made from stainless steel. An electrically isolating tape was applied to the stainless to prevent shorting the traces on the circuit boards. The sensor cap was very similar to chemiresistor cap, with slight modifications to allow for the larger SAW package. A PEEK manifold was bonded to the SAW socket rim. This manifold contained the geometry to accept a pre-concentrator. To date, however, the SAW device has not been tested with the pre-concentrator. Figure 6 shows the integrated SAW probe.

Figure 6. Integrated SAW probe for in-situ monitoring applications.

During testing of the SAW probe at the Nevada Test Site, several of the 32-gage wires broke during handling. As a result, several modifications were made to increase the ruggedness and functionality of the probe:

- Rotated circuit board bracket assembly 90° so that connector slot would not interfere with 4-40 screws
- Made small changes to bracket parts to allow to easier assembly, such as milled slot in washer to allow welding without fixtures
- Soldered cable wires directly to connector, rather than using 32 gage "intermediate wire" (that originally allowed for connector strain relief, but junctions were prone to failure)

2.2.3 Polymer Selection

The polymer selection was based on the work of Grate et al. (1995) and Abraham et al. (1994) who characterized 14 polymers and developed a methodology for estimating the responses of polymer-coated SAW sensors to a wide range of vapor phase analytes. They describe how to use linear solvation energy relationships (LSERs) to model the sorption of vapors by polymer layers. The overall sorption process (where the vapor is the solute and the polymer is the solvent) is modeled as a linear combination of particular interactions (e.g. polarity, acidity basicity). These solvation parameters have been determined for many organic solutes and the values for common chlorinated solvents important to DOE are shown in Table 1. Also shown in Table 2 are the solvation parameters for water because this is a potentially significant interfering species for environmental monitoring applications.

Table 2 lists the LSER experimentally determined coefficients for 14 polymers and oligomers of which some are commercially available but most are not. A polymer/vapor partition coefficient is estimated by combining the coefficients for a given polymer with the solvation parameters of a given vapor species. Table 3 lists the logarithm of the partition coefficients for the possible polymer/vapor combinations from Table 1 and Table 2.

Finally, Table 4 lists an estimated detection limit for a hypothetical SAW device for each of the targeted chlorinated VOCs with each of the 14 coating. The equation used to calculate these estimated detection limits is Equation 7 in Grate et al. (1995), but a coefficient of 2 was used rather than the coefficient of 4 as shown in the paper (personnel communication with Jay Grate, 2002). This calculation assumes a 500 MHz SAW device coated with a mass of polymer that shifts the frequency of the device by 1500 kHz and a detection sensitivity of 50 Hz. [Note that the SAW array devices used in this study registers a phase shift that produces a change in output voltage. The output voltage is not easily compared to a typical frequency-shift device. Approximate parameters for rough comparison are a polymer mass resulting in a 1-volt signal change and a detection sensitivity of 0.04 mV]

The purpose of Table 4 is to provide a rough relative comparison of the detection sensitivity of the 14 polymers for screening purposes. What is desired is a low estimated detection limit for a desired target VOC and a high detection limit for water, which generally acts as an interfering species. The polymer PVTD has the lowest (or next lowest) estimated detection limit for all of the VOCs of interest and a reasonably high detection limit for water. This polymer was also readily synthesized in-house at Sandia and was therefore chosen for use in this study. Two other polymers were also used. One is PIB, a commercially available polymer with reasonably low estimated detection limits for the targeted VOCs and the highest detection limit for water. The other polymer used was poly(ethylene vinyl acetate) (PEVA) which has been used with good success with the chemiresistor for monitoring these targeted VOCs but was not characterized by Grate et al. (1995) and therefore does not appear in these tables.

Table 1. Solvation parameters for selected chlorinated VOCs and water (from Abraham et al., 1994).

VOC →	PCE	TCE	t-1,2 DCE	c-1,2 DCE	1,1 DCE	CCl4	TCM	DCM	CM	water
R_2	0.639	0.524	0.425	0.436	0.362	0.458	0.425	0.387	0.249	0.000
π^H_2	0.420	0.400	0.410	0.610	0.340	0.380	0.490	0.570	0.430	0.450
$\Sigma\alpha^H_2$	0.000	0.080	0.090	0.110	0.000	0.000	0.150	0.100	0.000	0.820
$\Sigma\beta^H_2$	0.000	0.030	0.050	0.050	0.050	0.000	0.020	0.050	0.080	0.350
$Log\ L^{16}$	3.584	2.997	2.278	2.439	2.110	2.823	2.480	2.019	1.163	0.260
$Log\ L^W$	-0.070	0.320	0.570	0.860	-0.180	-0.060	0.790	0.960	0.400	4.640
V_x	0.837	0.715	0.592	0.592	0.592	0.739	0.617	0.494	0.372	1.028

Selected chlorinated VOCs: tetrachloroethene (PCE), trichloroethene (TCE), *trans*-1,2 dichloroethene (*t*-1,2 DCE), *cis*-1,2 dichloroethene (*c*-1,2 DCE), 1,1 dichloroethene (1,1 DCE), carbon tetrachloride (CCl4), trichloromethane (TCM), dichloromethane (DCM), chloromethane (CM).

Table 2. Linear solvation energy relationship (LSER) coefficients for 14 polymers and oligomers (from Grate et al., 1995).

	c	*r*	*s*	*a*	*b*	*l*
PIB	-0.766	-0.077	0.366	0.180	0.000	1.016
PECH	-0.749	0.096	1.628	1.450	0.707	0.831
OV25	-0.846	0.177	1.287	0.556	0.440	0.885
OV202	-0.391	-0.480	1.298	0.441	0.705	0.807
PVPR	-0.571	0.674	0.828	2.246	1.026	0.718
PVTD	-0.591	-0.016	0.736	2.436	0.224	0.919
PEM	-1.653	-1.032	2.754	4.226	0.000	0.865
SXCN	-1.630	0.000	2.283	3.032	0.516	0.773
PEI	-1.580	0.495	1.516	7.018	0.000	0.770
SXPYR	-1.938	-0.189	2.425	6.780	0.000	1.016
SXFA	-0.084	-0.417	0.602	0.698	4.250	0.718
FPOL	-1.207	-0.672	1.446	1.494	4.086	0.810
P4V	-1.329	-1.538	2.493	1.507	5.877	0.904
ZDOL	-0.486	-0.750	0.606	1.441	3.668	0.709

The polymers are fluoropolyol (FPOL), Fomblii-ZDOL (ZDOL), a 75% pheny1/25% methylpolysiloxane (OV25), an alkylaminopyridyl-substituted polysiloxane (SXPYR), poly(4-vinylheduorocumyl alcohol) (P4V), a hexafluoro-2-propanol-substituted polysiloxane (SXFA), poly(epichlorohydrin) (PECH), polybis(cyanopropyl)-siloxane (SXCN), poly(vinyl tetradecanal) (PVTD), poly(isobutylene) (PIB), poly(trifluoropropyl)methylsiloxane (OV-202), poly(ethylene maleate) (PEM), poly(vinyl propionate) (PVPR), and poly(ethylenimine) (PEI). The repeat unit of the structue of these polymers are shown in the cited reference.

Table 3. $\log K = c + r R_2 + s\pi^H_2 + a\Sigma\alpha^H_2 + b\Sigma\beta^H_2 + l\text{Log } L^{16}$ calculated from values in Table 1 and Table 2.

	PCE	TCE	t-1,2 DCE	c-1,2 DCE	1,1 DCE	CCl4	TCM	DCM	CM	water
PIB	2.9799	2.3994	1.6820	1.9215	1.4743	2.2060	1.9273	1.4821	0.5538	-0.1895
PECH	2.9744	2.5802	2.0181	2.5076	1.6280	2.2595	2.3820	2.0743	0.9980	1.6361
OV25	2.9795	2.4716	1.8450	2.2579	1.5450	2.2225	2.1469	1.8205	0.8159	0.5732
OV202	2.7397	2.3517	1.8505	2.2435	1.6146	2.1606	2.1226	1.8718	1.0426	1.0113
PVPR	2.7808	2.4757	1.9440	2.2775	1.5208	2.0792	2.2592	1.8873	0.8700	2.1891
PVTD	3.0016	2.6509	2.0279	2.3716	1.6037	2.2757	2.4118	1.9326	0.8082	2.0551
PEM	1.9444	1.8383	1.3884	2.1516	0.7349	1.3628	2.0370	1.6864	0.2802	3.2765
SXCN	2.0993	1.8579	1.3656	2.0073	0.8031	1.4197	1.8708	1.5610	0.2920	2.2652
PEI	2.1327	2.1549	1.6376	2.2106	0.7393	1.3965	2.3355	1.7321	0.0906	5.0572
SXPYR	2.6011	2.5203	1.9006	2.6827	0.9618	1.7651	2.7066	2.1004	0.2393	4.9770
SXFA	2.4757	2.2735	1.8965	2.1419	1.6972	1.9807	2.0041	1.8297	1.2461	2.4334
FPOL	1.8740	1.6889	1.2842	1.7263	0.9548	1.3213	1.5306	1.3462	0.5164	2.3095
P4V	1.9752	1.8684	1.5283	2.1856	1.1632	1.4659	1.8244	1.7665	0.8815	3.3206
ZDOL	1.8303	1.7136	1.3719	1.6278	1.1279	1.4023	1.5400	1.3281	0.7058	2.4365

Table 4. Polymer detection estimate in ppm_v calculated using: $C_v = \Delta f_v / (2\Delta f_s K/\rho_s)$[*] (Adapted from Grate et al., 1995).

VOC		PCE	TCE	c-1,2 DCE	t-1,2 DCE	1,1 DCE	CCl4	TCM	DCM	CM	water
Mwt →		165.83	131.4	96.94	96.94	96.94	153.8	119.5	85.0	50.4	18.0 (g/mol)
Polymer	ρ_s (g/cm³)										
PIB	0.918	2.4	11.3	80.3	46.2	129.5	15.1	37.0	145.0	2073.5	32152.0
PECH	1.360	3.5	11.1	54.8	17.8	134.6	19.8	19.2	54.9	1104.7	711.6
OV25	1.150	3.0	12.0	69.1	26.7	137.8	18.3	28.0	83.3	1420.5	6955.9
OV202	1.252	5.6	17.3	74.3	30.0	127.8	22.9	32.2	80.6	917.7	2761.5
PVPR	1.010	4.1	10.5	48.3	22.4	128.0	22.3	19.0	62.8	1101.6	147.9
PVTD	0.960	2.4	6.7	37.8	17.2	100.5	13.5	12.7	53.7	1207.0	191.4
PEM	1.353	37.8	60.9	232.6	40.1	1047.0	155.5	42.4	133.5	5737.4	16.2
SXCN	1.120	21.9	48.2	202.9	46.3	740.9	112.9	51.4	147.5	4622.9	137.7
PEI	1.050	19.0	22.8	101.7	27.2	804.4	111.6	16.5	93.3	6889.9	0.2
SXPYR	1.000	6.2	9.4	52.8	8.7	458.9	45.5	6.7	38.0	4659.8	0.2
SXFA	1.477	12.1	24.4	78.8	44.8	124.7	40.9	49.9	104.8	677.6	123.2
FPOL	1.653	54.3	104.9	361.1	130.5	771.1	209.0	166.1	357.0	4069.8	183.5
P4V	1.440	37.5	60.5	179.3	39.5	415.7	130.5	73.6	118.2	1529.3	15.6
ZDOL	1.800	65.4	107.9	321.3	178.3	563.6	188.9	177.0	405.3	2864.9	149.2

[*]per personal discussions with Jay Grate, a coefficient of 2 was used rather than the coefficient of 4 shown in Eqn 7 of Grate et al. (1995). Calculation basis: P=1 atm, T=25 C, Δf_s mass load=1500 kHz, Δf_v min signal=50 Hz.

2.3   Calibration

The chemiresistor and SAW sensors were calibrated using controlled concentrations of TCE. The sensors were both placed in customized six-inch steel tubes that allowed the sensors to be exposed to a flowing stream of varying concentrations of TCE vapor. Data were logged using either a Campbell Scientific CR23X or an Agilent 34970A multiplexer. Figure 7 shows a schematic of the apparatus used for the calibrations.
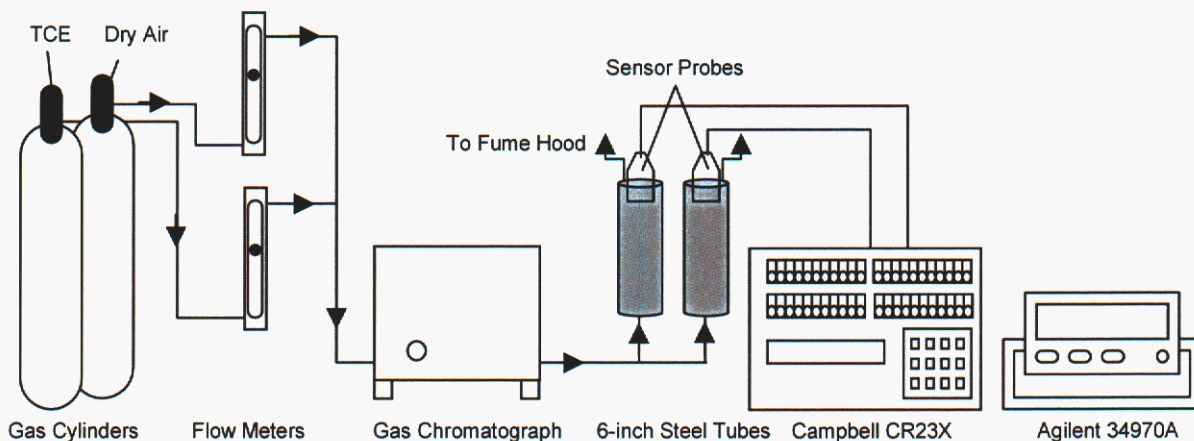
Figure 7. Schematic of apparatus for calibration experiment.

For the initial calibration runs, the sensors were connected to the Campbell CR23X, which was programmed to read the chemiresistor signal in ohms and the SAW signal in DC volts. The CR23X was used for the calibration runs because it was the same datalogger that was to be used in the field tests at the Nevada Test Site (later calibrations and analyses were also conducted using the Agilent 34970A; see Appendix A). The SAW device required 3.3 V of input, so it was powered for approximately 2 hours prior to the beginning of the calibration run to ensure ample warm-up time. Dry air was passed across each sensor in order to remove the water vapor, and the sensors were allowed to reach equilibrium in the dry conditions. When the measured resistances and voltages were stable, the baseline was recorded and the calibration commenced. TCE vapor concentrations of 500, 1000, 5000, and 10,000 ppmv (parts per million by volume) were exposed to the sensors using customized gas cylinders containing 1,000 and 10,000 ppmv of TCE (500 and 5,000 ppmv were achieved through dilution with dry air from a compressed gas cylinder). TCE concentrations was measured using an MTI M200™ micro-gas chromatograph. Following each exposure, dry air was used to purge the sensor and allow a new baseline to be established for the next exposure. The relative changes in resistance (for the chemiresistor) and voltage (for the SAW) were used in the calibrations. The relative change is calculated as the maximum change in resistance (or voltage) divided by the baseline resistance (or voltage) for

each exposure (see Table 5). The baseline value, R_b, is calculated as a two-minute average prior to exposure to TCE. The maximum change is calculated by taking the difference between the baseline value and a value averaged for two minutes prior to shutting the TCE off. The TCE was turned off after the sensors had stabilized, which typically took 15-20 minutes. The relative changes in sensor signals ($\Delta R/R_b$ or $\Delta V/V_b$) were then plotted against the TCE concentration for each exposure using Microsoft Excel, and regressions were fit to points. Figure 8 shows the results from the calibration run for the chemiresistor E2, which contained the following polymers: polyepichlorohydrin (PECH), poly(N-vinyl pyrrolidone) (PNVP), polyisobutylene (PIB), and poly(ethylene-vinyl acetate) copolymer (PEVA).

Table 5. Equations for calculating the normalized change for the chemiresistor and SAW.

Chemiresistor	SAW
$(R-R_b)/R_b$	$(V-V_b)/V_b$
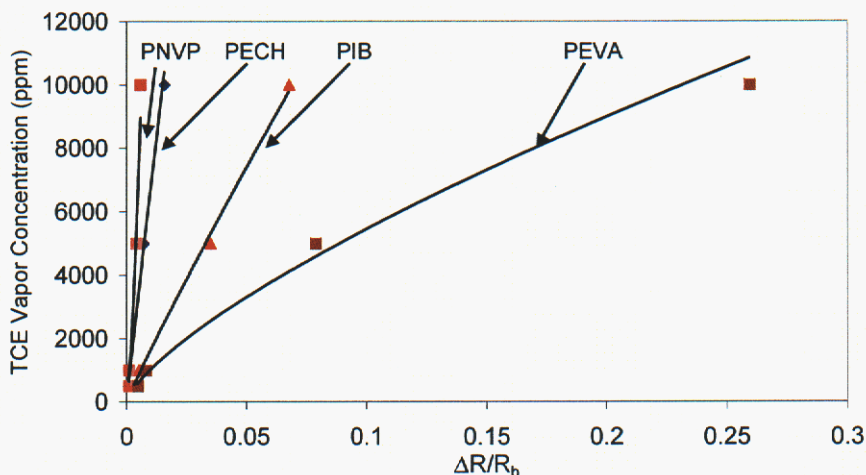
Figure 8. Graph of the calibration of chemiresistor E2 to TCE under dry conditions at room temperature, 23 C.

All of the polymers on the chemiresistor responded to the different concentrations of TCE. Graphical analysis of the data shows that the chemiresistor E2 can be best fit with a power function. Table 6 shows the power functions for each polymer on the chemiresistor.

Data for the SAW sensor P9 was analyzed and graphed in a similar manner. Figure 9 shows the results of the calibration run for SAW P9, which contained the following polymers: polyisobutylene (PIB) and two channels with poly(vinyl tetradecanal) (PVTD).
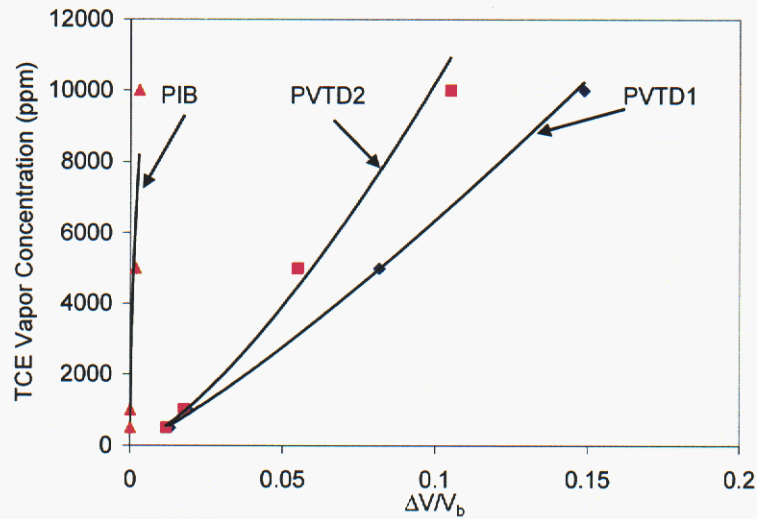
Figure 9. Graph of the calibration of the SAW P9 to TCE under dry conditions.

The polymer PVTD appeared responsive for the calibration runs. However, the polymer PIB on the SAW did not elicit a strong response to TCE. The responses of the polymers were fitted with a power function, and Table 6 shows the power functions for the polymers on SAW P9.

Table 6. TCE calibrations for chemiresistor E2 and SAW P9 at room temperature (23 °C) in dry conditions.

|	Polymer	Regression Type	Regression (ppm)	R^2	Regression (g/L)	R^2
Chemiresistor E2	PECH	Power	$y_1 = 5.45E{+}05x^{9.51E\text{-}01}$	0.972	$y_2 = 2.46E{+}00x^{9.51E\text{-}01}$	0.972
	PNVP	Power	$y_1 = 1.71E{+}07x^{1.45E{+}00}$	0.935	$y_2 = 7.71E{+}01x^{1.45E{+}00}$	0.935
	PIB	Power	$y_1 = 1.19E{+}05x^{9.28E\text{-}01}$	0.993	$y_2 = 5.39E\text{-}01x^{9.28E\text{-}01}$	0.993
	PEVA	Power	$y_1 = 2.87E{+}04x^{7.21E\text{-}01}$	0.991	$y_2 = 1.30E\text{-}01x^{7.21E\text{-}01}$	0.991
SAW P9	PVTD1	Power	$y_1 = 1.00E{+}05x^{1.20E{+}00}$	0.995	$y_2 = 4.53E\text{-}01x^{1.20E{+}00}$	0.995
	PVTD2	Power	$y_1 = 2.44E{+}05x^{1.38E{+}00}$	0.995	$y_2 = 1.10E{+}00x^{1.38E{+}00}$	0.995
	PIB	Power	$y_1 = 2.02E{+}05x^{5.48E\text{-}01}$	0.936	$y_2 = 9.13E\text{-}01x^{5.48E\text{-}01}$	0.936

y_1 = TCE vapor concentration (ppmv)
y_2 = TCE vapor concentration (g/L)
$x = \Delta R/R_b$ for chemiresistor; $\Delta V/V_b$ for SAW

22

2.4 SAW Optimization

A recent report from the GE Research & Development Center (Potyrailo et al., 2001) describes their efforts to dramatically increase the sensitivity of an acoustic wave sensor. They found that optimal performance was achieved by optimizing both the gate time, over which the data was averaged, and the thickness of the polymer coating. Control over the gate time, or the number of sensor readings used in a running average, was easily achieved with our data logger and thus was the focus of our optimization efforts for the NTS field test. Control of the polymer coating thickness is more difficult.

Utilizing the standard picospritzed technique, three SAW arrays were coated with PIB and PVTD. Only qualitative efforts were made to optimize the coatings, and the surface of the coatings were visibly rippled when viewed under a microscope as shown in Figure 10. It is postulated that this rippled surface primarily results from the rapid evaporation of the solvent. Slowing the solvent evaporation may allow the polymer surface to flatten before it sets. A rippled surface necessarily means there is a variation in the coating thickness; thus, an optimal thickness is difficult to achieve.
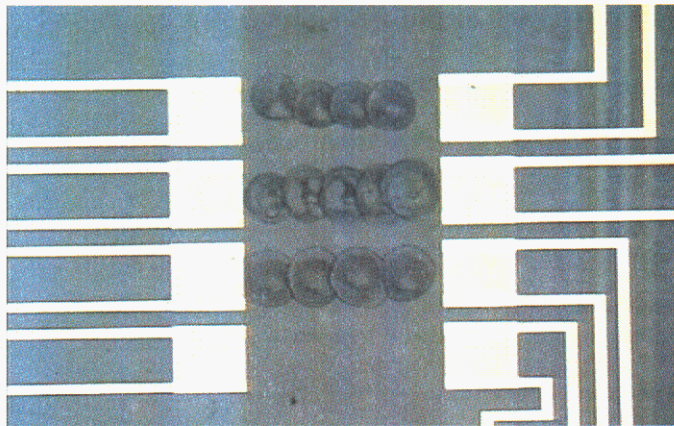

Figure 10. Polymer coating on SAWs sensor as applied by the standard picospritzer technique. Note the ripples on the resulting surface.

Figure 11 shows the output of one sensor when exposed to 1000 ppmv and 10,000 ppmv TCE calibration gases. This data was collected at a rate of 5 samples per second, the maximum rate achievable with our data-acquisition system. The standard deviation of the noise is about 0.13 mV which is within the expected range of 0.05 to 0.15 mV. However, the response or sensitivity to TCE was much lower than expected. As speculated, the PVTD coated sensor was more sensitive to TCE than the PIB coated sensor. The PVTD coating resulted in only a 1 mV signal when exposed to a 1000 ppmv TCE calibration gas and only about a 10 mV signal when exposed to a 10,000 ppmv TCE calibration gas.

**0.2 sec data acquisition, std dev 0.000127 V**
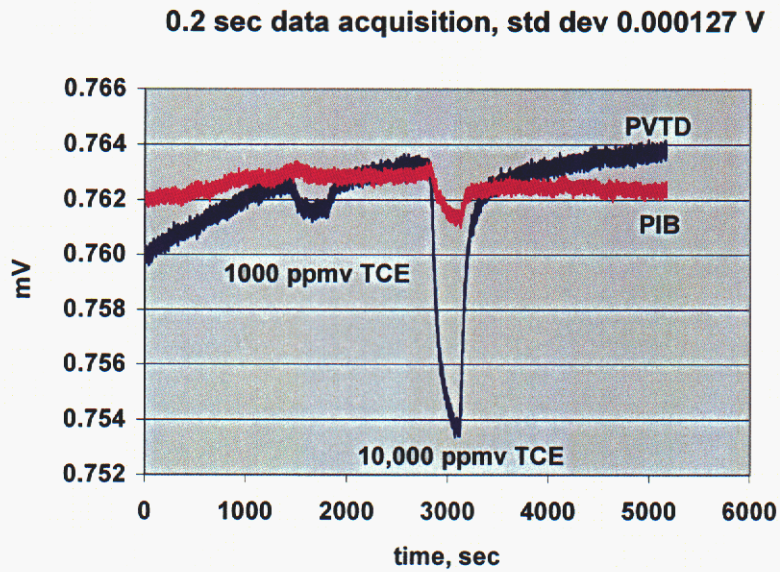
Figure 11. Output of SAWs sensor when exposed to 1000 and 10,000 ppm TCE. Data acquired at a rate of 5 samples per second.

Figure 12 shows the same data processed as a running average using a time window or gate of 120 seconds (600 data points). As the gate time was increased, the standard deviation of the sensor noise decreased. The detection limit can be estimated by extrapolating the 1000 ppmv TCE response linearly to zero and defining the detection limit at three standard deviations above the noise. Figure 13 shows the estimated detection limit as a function of the number of data points used in the running average. The detection limit was improved by just over an order of magnitude, which is similar to the improvement demonstrated in the GE study.

**120.0 sec running average, std dev 0.000012 V**
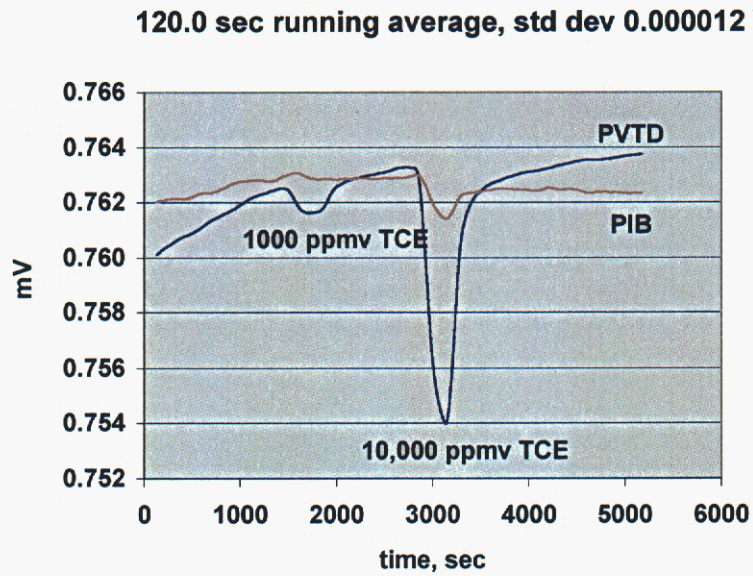
Figure 12. Data of Figure 11 processed as a 120-second running average.
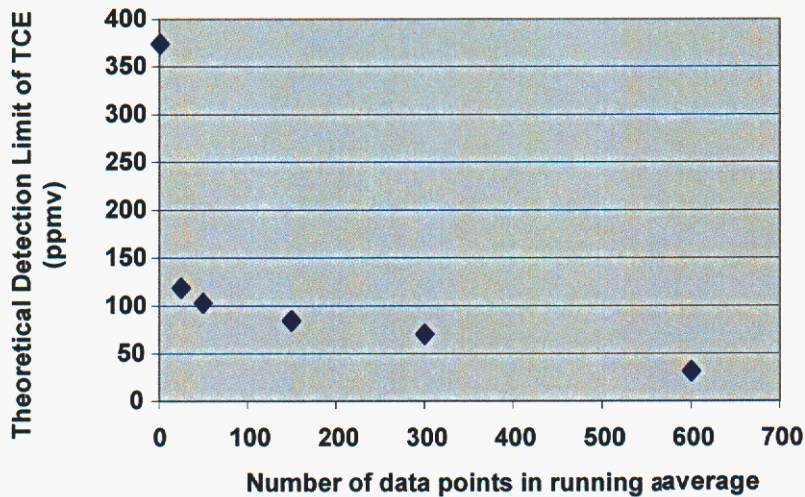
Figure 13. Estimated detection limit of SAW sensor for TCE as a function of the size of the running average.

In preparation for the NTS field test, the Campbell Scientific datalogger was programmed to perform a running average of the SAW-sensor output and record only the average. Due to the complexity of the data-acquisition program (for collecting the SAW data, chemiresistor data, as well as number of environmental parameters) the SAW sensor could only be read every 0.4 seconds and the averaging window was limited to 100 samples. Figure 14 shows the calibration curves for the three sensors on the SAWs array presently in use at the NTS field test. It should

25

be noted that this is a different SAWs array than that used in the noise testing discussed above. Two of the sensors are coated with PVTD and one is coated with PIB. A four-point calibration was performed using nominally 500, 1000, 5,000 and 10,000 ppmv TCE calibration gas (the concentration of the calibration gas was independently monitored with a gas chromatograph). The PIB sensor showed very little sensitivity to TCE. One of the PVTD sensors was clearly more sensitive than the other and was about twice as sensitive as the one used in the noise testing. The calibration curve for the superior PVTD sensor fit very well to a power law function. The estimated detection limit for the better PVTD sensor is 10 to 20 ppmv TCE. We hope to achieve up to an order of magnitude sensitivity improvement by optimizing the coating layer thickness, which will require modifications to the coating process such that a smooth surface is produced.

Absolute Value (DmV/mVb) 9-18-02 Temp 23C Dry
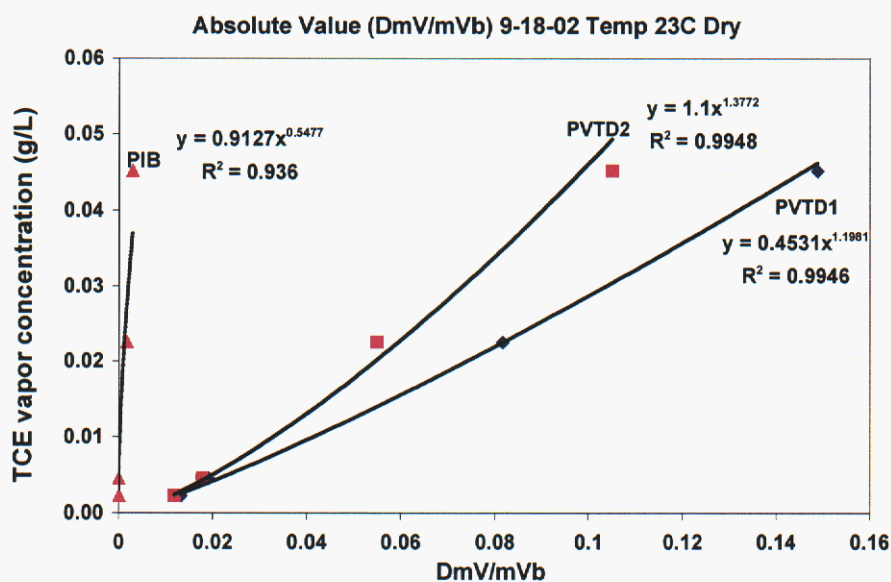
Figure 14. Calibration curves for SAW sensor used in the NTS field test.

2.5   *Theoretical Limits of Detection*

In order to calculate the theoretical limit of detection, the noise of the SAW and chemiresistor were analyzed during operation. The theoretical limit of detection was defined as the minimum analyte concentration that caused a change in resistance or voltage that was three standard deviations greater than the noise.

The following procedure was followed to determine the theoretical limits of detection. First, the mean and standard deviation was calculated during a quiescent (no exposure) period of data for the chemiresistor and SAW sensors. Second, the standard deviation was multiplied by three and then divided by the mean in order to find the relative change in resistance or voltage that corresponded to the theoretical detection limit. These values were then entered into the TCE calibration for the sensor (Table 6) to determine the theoretical concentration detection limit. This process was repeated multiple times to generate statistics on the theoretical limit of

detection, and Table 7 summarizes the results for chemiresistor E2 and SAW P9. Figure 15 shows a bar graph of the limits of detection.

Table 7. Theoretical limits of detections for chemiresistor E2 and SAW P9.

|	Polymer	Mean,μ (ohms/volts DC)	Limit of Detection (TCE ppm)	Standard Deviation of Limit of Detection (TCE ppm)
Chemiresistor E2	PECH	285.3	63.8	6.3
	PNVP	262.4	386.0	164.5
	PIB	445.8	22.3	17.6
	PEVA	409.0	67.0	57.7
SAW P9	PVTD1	123.3	25.3	15.7
	PVTD2	217.0	4.3	0.5
	PIB	-835.6	691.5	278.7
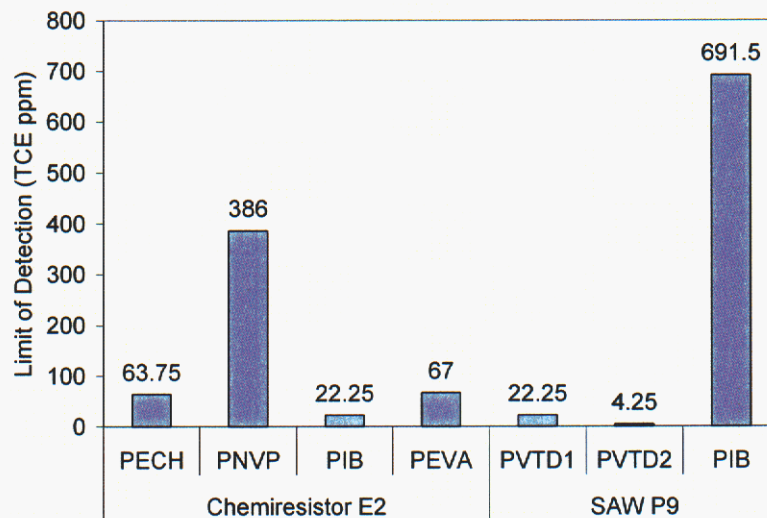
Figure 15. Theoretical limits of detection for chemiresistor E2 and SAW P9.

The same procedure was followed for chemiresistor E19, which contains the polymer PVTD. The purpose was to compare the theoretical detection limits using the same polymer on both the chemiresistor and SAW sensor. Table 8 and Figure 16 summarize the limits of detections for the polymers on chemiresistor E9.

Table 8. Theoretical limits of detection for chemiresistor E19.

|	Polymer	Mean, μ (ohms)	Limit of Detection (TCE ppm)	Standard Deviation of Limit of Detection (TCE ppm)
	PECH	130.6	40.4	13.6
Chemiresistor E19	PNVP	102.2	436.2	310.0
	PVTD	233.4	4.8	3.7
	PEVA	233.4	14.6	5.5
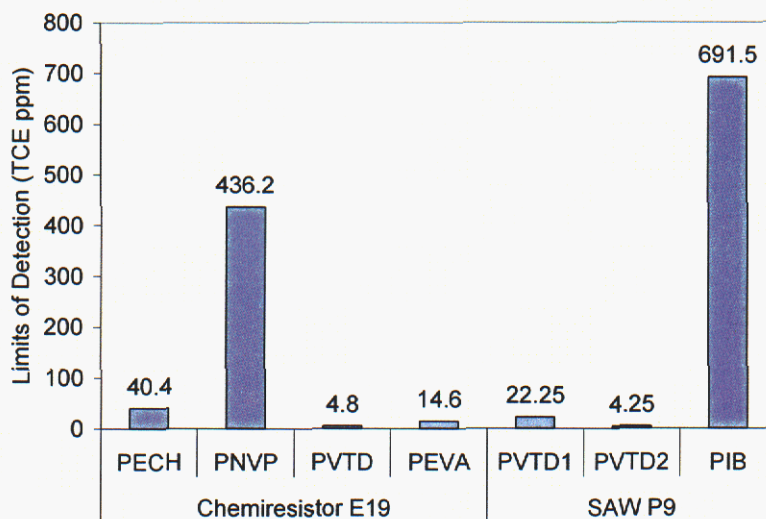
Figure 16. Theoretical detection limits for chemiresistor E19 and SAW P9.

3. Field Tests

The field tests were performed at the HAZMAT (Hazardous Materials) Spill Center (HSC) at the Department of Energy's Nevada Test Site, located about 120 km (75 miles) northwest of Las Vegas, NV. The HSC is a unique facility built to conduct tests with hazardous materials for research and training purposes. The HSC Environmental Impact Statement allows releases of high concentrations of hazardous materials for both large- and small-scale testing.

3.1   55-Gallon Drum Test

The 55-gallon drum test consisted of a 200 L (55 gallon) drum that was filled with moist sand.[1] A slotted PVC tube was placed vertically in the center of the drum to act as a contaminant reservoir. A slotted and screened 7.6 cm diameter steel tube was placed 20 cm away from the reservoir to simulate a well. The sensor package (chip B11, all PEVA) was suspended midway down the steel tube (~36 cm), and the cable was threaded through a port in the drum to an Agilent 34970A data-acquisition unit in a nearby trailer. The data-acquisition unit was connected to a laptop that used the Agilent Benchlink Data Logger software (v. 1.4). Figure 17 shows a top view of the open drum, exposing the tops of the contaminant reservoir and screened well.
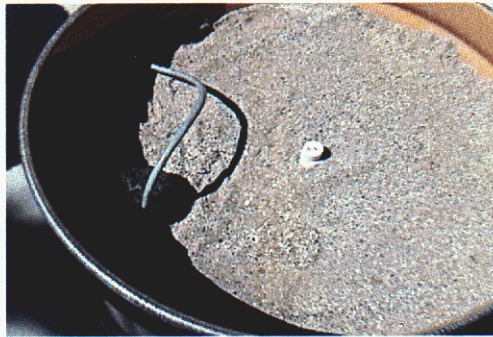
Figure 17. Top view of 55-gallon drum filled with sand. The contaminant reservoir is in the middle of the drum, and the sensor well (with sensor cable) is towards the outside.

3.1.1 Approach

The experiment consisted of three phases: (1) a period of ambient background data logging for nearly four days to observe the impacts of diurnal temperature variations on the system; (2) emplacement of TCE into the contaminant reservoir; and (3) remediation using compressed air to vent the sand for a brief period. During the ambient logging, the drum was completely sealed while data were logged. After the ambient period, approximately 60 mL of TCE was emplaced in the contaminant reservoir. Approximately 35 mL was absorbed onto a wick that was placed in the reservoir, and 25 mL was poured into and around the reservoir. During the simulated remediation process, the lid of the drum was removed and a compressed air tank was used to blow air (~10 L/min) through four equally spaced ports around the bottom perimeter of the drum. The air flowed through the contaminated sand and through the open top of the drum. During all phases, a tarp was draped around the drum to shade the drum from direct sunlight. Figure 18 shows a photograph of the experiment.

---

[1] Measured sand properties: grain density=2.3 g/mL; porosity=0.39; saturation=0.18; variable grain size.
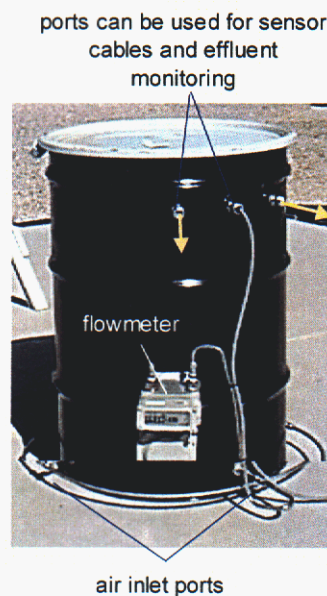
Figure 18. Photograph of the exterior of the sand-filled drum.

3.1.2 Results

3.1.2.1 Ambient Background Data Logging

During the ambient background data-logging period, the temperature sensor on the chip indicated that the temperature oscillated between approximately 20°C to 30°C because of the diurnal heating and cooling. The chemiresistor also showed a response that closely resembled the temperature variations. As the temperature increased, the polymers swelled due to thermal expansion, which increased the measured resistance. As the system cooled overnight, the polymers shrunk, and the measured resistances of the chemiresistors decreased as the carbon particles that were separated were brought into contact again. These temperature variations and their affect on the "baseline" chemiresistor resistance pose an issue for calibrations at low chemical concentrations, but at higher concentrations, the magnitude of the increased resistance overwhelms the variations caused by temperature. Figure 19 shows the response of one of the four chemiresistor sensors during the ambient period, along with the temperature. All four chemiresistors behaved similarly; therefore, only the results from one chemiresistor ("sensor 3") are shown in the resulting plots for clarity.

In addition to the diurnal fluctuations, Figure 19 shows that the response of the chemiresistor exhibits a long-term drift towards higher resistances. We speculate that the drift is caused by a continual exposure to large water-vapor concentrations (nearly 100% relative humidity between 20°C and 30°C). Significant drift was not observed for similar chemiresistors stored in the laboratory for long periods of time.

Another interesting observation during the ambient period was that significant amounts of water condensed in the drum as the system cooled overnight. The liquid water was observed in large amounts on the lid, along the walls of the steel well (which showed evidence of rusting), and on

30

the sensor package and cable. However, after unscrewing the sensor package, we observed that the chip and chemiresistors inside were dry and did not appear to show any signs of deterioration.
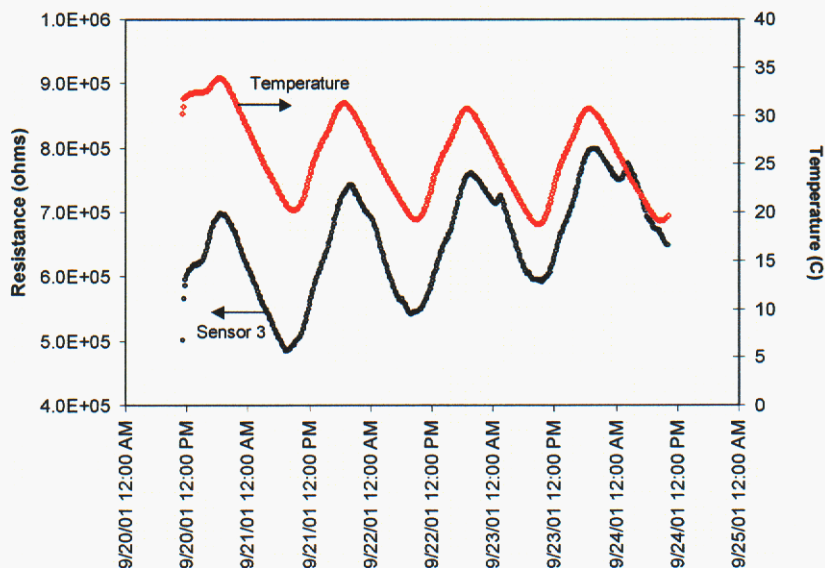

Figure 19. Plot of chemiresistor temperature and resistance during the four-day ambient data-logging period.

3.1.2.2   TCE Emplacement and Ventilation

Following four days of ambient data logging, TCE was emplaced into the contaminant reservoir. The sand was then ventilated after the sensor responded to the presence of TCE. Figure 20 shows a plot of the logged data during the TCE emplacement and ventilation periods, along with the data from the last day of the ambient period for reference and scaling. The chemiresistor shows a drastic increase in resistance only a few minutes after the TCE was emplaced. The resistances increased to greater than 100 MΩ, which was the maximum limit on the data acquisition unit. The rapid detection of TCE by the chemiresistor sensor was somewhat surprising. Past studies have shown that diffusion-limited transport should have resulted in a much longer time until breakthrough (several hours).[3] We believe that the rapid breakthrough observed in this test may have been due to the liquid TCE that was poured around the contaminant reservoir. The liquid may have spread as it migrated downward under the force of gravity, possibly coming quite close to the sensor located in the well 20 cm away from the contaminant reservoir and 36 cm below the sand surface.

After about four hours, the lid was removed and compressed air was forced through the sand from the bottom via the venting ports for about 45 minutes. Figure 20 shows that the chemiresistor resistances dropped significantly during the purging of clean air through the system. After the ventilation was stopped, the lid was closed and the resistances began to increase again due to exposure to residual TCE remaining in the sand.

31
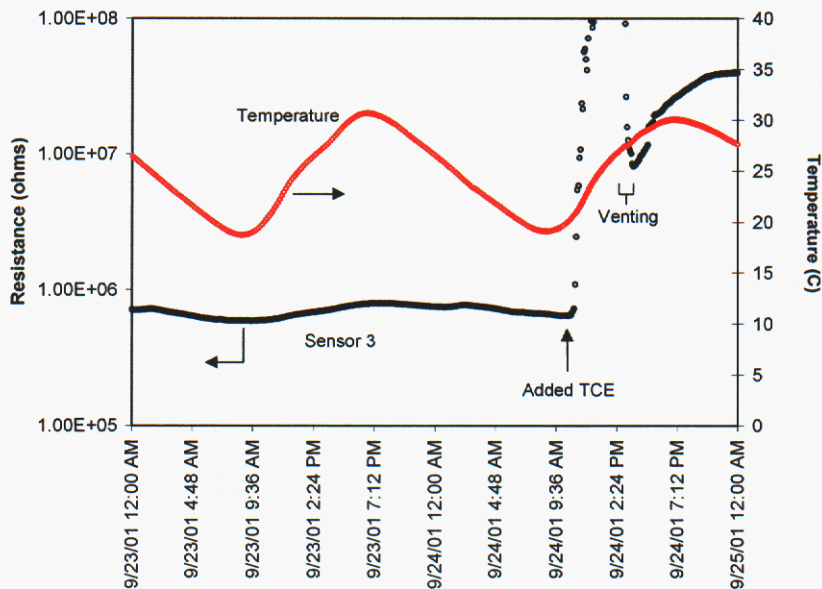
Figure 20. Plot of chemiresistor temperature and resistance during TCE emplacement and ventilation periods. Note that the resistances are clipped at 100 MΩ, which is the maximum readout of the data logger.

3.1.2.3 Data Analysis

The chemiresistor resistances plotted in Figure 20 can be transformed to TCE concentrations using the following steps to apply correction factors and calibration curves:

1. Remove the effects of drift by applying an appropriate correction factor derived from a regression between measured resistance (at a prescribed temperature) and time during the ambient background period.

2. Remove the effects of temperature/water-vapor-concentration fluctuations by applying an appropriate correction factor derived from a regression between measured resistance and temperature during the ambient background period.

3. Apply a calibration curve (TCE concentration vs. relative change in resistance) to the temperature- and drift-corrected resistances to obtain a TCE concentration for each data point.

Because no TCE was present during the ambient period, we can assume that the changes in resistance during this period are due entirely to drift, temperature variations, and/or changes in water-vapor concentrations (caused by changes in temperature). To account for drift, the measured resistances at a prescribed temperature 86°F (30°C) were plotted as a function of elapsed time since the start of the experiment during the ambient period. These values can be

32

identified in Figure 19 by selecting resistance values that correspond to a chip temperature of 86°F (30°C). A linear regression was fit to the data (with a correlation coefficient of 0.96) and the slope (4.88×10^4) was applied in the following expression to correct for drift:

$$R_D = R - 4.88 \times 10^4 t \qquad (1)$$

where R_D is drift-corrected resistance (ohms), R is the measured resistance (ohms), and t is the elapsed time (days). The measured resistances are corrected for drift by multiplying the elapsed time when each resistance was measured (starting at time zero at the beginning of the experiment) by the slope of the linear regression and subtracting this "drift-induced" change in resistance from the measured resistances.

A similar procedure was performed to correct for temperature and water-vapor-concentration variations. Because the sand used in the experiment was moist, we assumed that the relative humidity was always at 100%. Therefore, the water-vapor concentration was perfectly correlated to the system temperature, and impacts on the chemiresistor response caused by fluctuations in water-vapor concentrations could be combined with the impacts caused by fluctuations in the system temperature. The chemiresistor resistance was plotted as a function of system temperature during the ambient period, and the slope of the linear regression (1.459×10^4; correlation coefficient = 0.89) was applied in the following expression to account for fluctuations in temperature and water-vapor concentration:

$$R_T = R_D - (T - T_{ref}) \times 1.459 \times 10^4 \qquad (2)$$

where R_T is the corrected resistance for the combined impacts of temperature, water-vapor concentration, and drift (ohms); T is the measured temperature (°C); and T_{ref} (°C) is a reference temperature that was used for the calibrations (23 °C or 73 °F). If the measured temperature at any point in time is greater than (or less than) the reference temperature, than a temperature-induced change in resistance will be subtracted (or added) to the drift-corrected resistance.

The chemiresistor sensors that were used in the experiment were calibrated to known concentrations of TCE. A power-law curve fit was used to correlate the relative change in resistances to the TCE concentrations. The resulting curve fit (using calibrations after the test) for sensor 3 is given as follows with a correlation coefficient of 0.97:

$$C = 0.0034 x^{0.4092} \qquad (3)$$

where C is the TCE vapor concentration (g/L; can be converted to lbm/ft^3) and x is the percent relative change in resistance ($[R_T - R_b]/R_b$, where R_b is the average corrected baseline resistance during the ambient period (5.16×10^5 ohms). The following expression is then used to convert the TCE vapor concentration to units of parts per million (C_{ppm}):

$$C_{ppm} = \frac{CRT^o}{P_{atm}} \times 10^6 \qquad (4)$$

where R is the gas constant for TCE (63.5 J/kg-K or 11.8 ft-lbf/lbm-R), T^o is the absolute system temperature (Kelvin or Rankine), and P_{atm} is the local atmospheric pressure (90 kPa or 13 psia).

The chemiresistor-resistance values shown in Figure 20 are re-plotted in Figure 21 using Equations (1)-(4). The normalized concentrations are also plotted using the saturated TCE vapor concentration (calculated at each measured temperature) as the normalization factor. Despite the correction factors, the impacts of diurnal fluctuations are still evident during the ambient period. We noted that the correlation between chemiresistor resistance and temperature exhibited some hysteresis during the heating and cooling cycles, and this may have impacted our ability to completely remove the effects of diurnal fluctuations. The diurnal fluctuations during the ambient period resulted in calculated TCE vapor concentrations that varied by several thousand parts per million (ppm). The maximum TCE vapor concentration recorded after the contaminant was emplaced (before being clipped by the data logger) was approximately 50,000 ppm, which corresponds to nearly 40% of the saturated TCE vapor concentration.

In this analysis, independent univariate regression methods were used to calculate TCE concentrations from the measured resistances. The effects of drift, temperature, and water-vapor concentration were assumed to be independent. More rigorous multivariate regression methods need to be considered to account for the correlations and interdependencies among the various inputs.
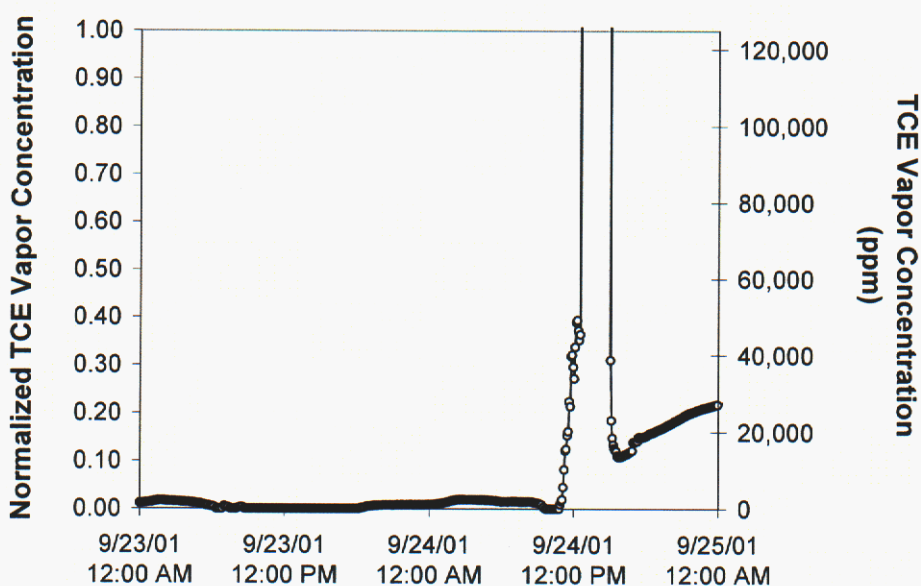
Figure 21. Calculated gas-phase TCE concentrations using Equations (1)-(4) and the resistances from chemiresistor sensor 3.

3.2   Sandbox Test

3.2.1   Test Description

The Sandbox Test consisted of a 4' x 4' x 2' steel container that was filled with dry 20-40 mesh sand. Several PVC tubes (2" ID) were placed vertically in the sand for sensor and contaminant emplacement (see Figure 22). The chemiresistor sensor was placed in a vertical tube 25 cm away from the center. Additional sensors were placed in the tube along with the chemiresistor to record the barometric pressure, temperature, and humidity (see Figure 23). In the experiments, trichloroethylene (TCE) was absorbed into a wick and then placed in the central tube (see Figure 24). The sandbox was then insulated and data were recorded as the TCE vapors diffused through the sand to the sensors.   Two tests were performed—one from May to June, 2002, and another from September to December, 2002.

The sensors were connected via cable to a Campbell CR-23X data logger that was powered by a solar panel. A cell phone was connected to the data logger so that data could be downloaded remotely. During the experiment, the data were also posted in real time to web sites so that the response of the sensors could be tracked continuously.   The primary difference between this test and the 55-gallon-drum test was the inclusion of data-acquisition and telemetry instrumentation that could be operated remotely and autonomously. We wanted to demonstrate the ability to operate, monitor, and post data from the sensors continuously using commercial products in a remote environment.

Figure 22. Sandbox Test. Left: Placement of tubes for contaminant (center tube) and sensors.
Right: Sandbox with data-logging station in background.
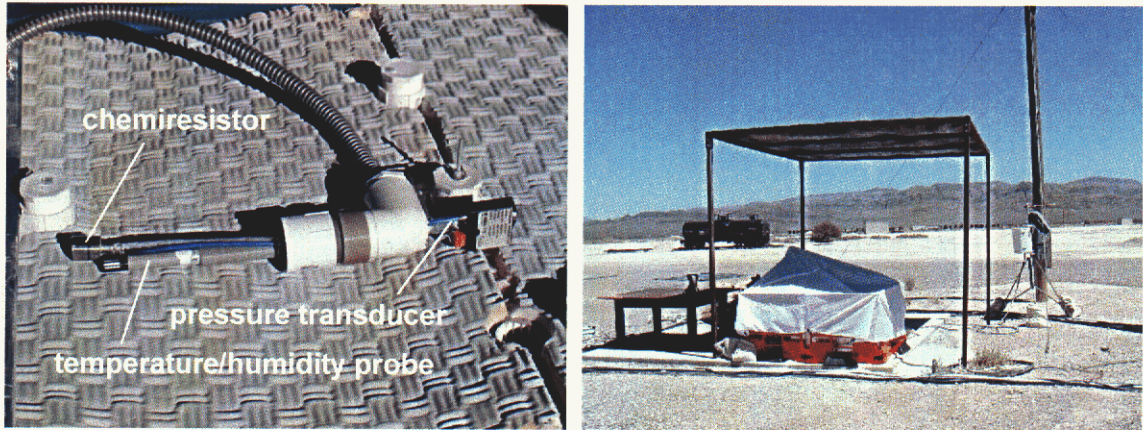
Figure 23. Left: Sensors emplaced in the sandbox. Right: Sandbox shaded from sun.
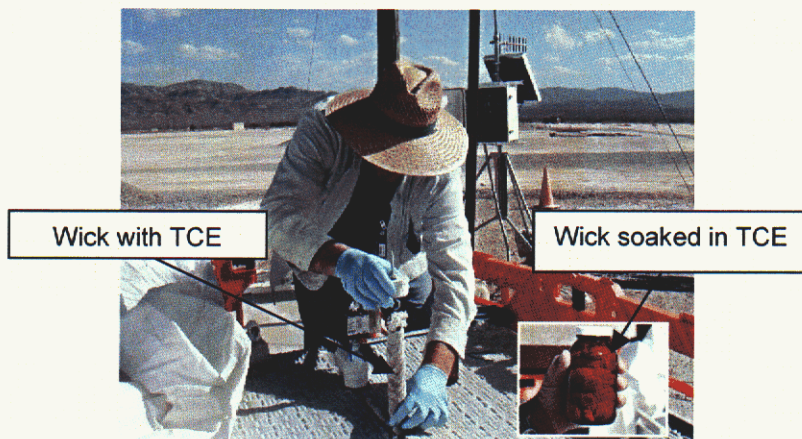
Figure 24. Emplacement of TCE into the sandbox.

3.2.2 Data Acquisition and Telemetry

Requirements

An instrument and associated software product was needed that could record five resistance measurements and three voltage measurements, operate in a remote location, and provide environmental (temperature, relative humidity, and barometric pressure) data through external and internal sensors.

The Campbell Scientific, Inc., CR23X Micrologger® was utilized based on the above requirements. The CR23X provides 12 differential or 24 single-ended, individually configured

voltage measurements. The accuracy, range, and resolution are as follow (Campbell Scientific, Inc, LoggerNet Instruction Manual, 1999-2002):

ACCURACY: ±0.025% of FSR, 0° to 40°C
±0.05% of FSR, -25° to 50°C
±0.075% of FSR, -40° to 80°C;(-XT only)
Note: ±5 µV offset voltage error is possible with single-ended (SE) measurements.

RANGES AND RESOLUTION:

Input Range (mV)	Resolution (µV) Diff.	Accuracy (mV) SE	(-25° to 50°C)
±5000	166 333	±5.00	
±1000	33.366.6	±1.00	
±200	6.6613.3	±0.20	
±50	1.673.33	±0.05	
±10	0.330.66	±0.01	

The Campbell Scientific MSX10 solar panel with the BP24 24-Amp-hour battery pack were installed to address remote power requirements. The battery pack was later exchanged for the USRM22NF 60-Amp-hour battery pack due to concerns of possible long-term low-peak power (overcast) days. The COM100 cellular phone package was chosen for its CR23X compatibility and to alleviate issues associated with RF telemetry and the lack of standard phone line availability.

The temperature, relative humidity, and barometric pressure were recorded by employing a CR23X compatible HX94 Temperature/RH Probe along with a PX215 Pressure Transducer manufactured by Omega® Engineering Inc.

Telemetry

Telemetry was accomplished by utilizing the PC208(W) software package combined with a cellular transceiver and an external RJ11C telephone interface. A computer with PC208(W) software and a Hayes-compatible phone modem was connected to a standard phone line and used to call the cellular equipped data-logging station. PC208 was used to upload programs written by the user to record, process, and log the necessary data (see Appendix B).

Power Requirements

Power requirements were calculated to assure that the power source (solar panel) would be able to supply the appropriate amount of current under adverse (cloudy) conditions (see Table 9). Table 10 shows the battery life if the solar panel were not able to recharge the battery for a length of time due to adverse conditions. Figure 25 and Figure 26 show the battery voltage during month-long tests of the system. Both appear to perform adequately, but the 60-amp-hour battery appears to provide a more consistent and stable level of power to the data-logging station for extended periods of time.

Table 9. Power requirements for the CR23X data-logging station (worst-case scenarios).

	Hours	Amps	Amp-Hr/Day
SAW	24	0.09	2.16
Chemiresistor	N/A	N/A	N/A
Cell Phone (Stand By)	15	0.17	2.55
Cell Phone (On-line)	.2	1.8	0.36
HX941 Temp/Rh Probe	24	0.02	0.48
PX215 Pressure Probe	24	0.02	0.48
CR23X Micrologger®			
Processing	2	.1175	.235
Quiescent	22	.0025	.055
Total			6.32

Table 10. Solar panel with battery pack specifications.

	Current @ peak Power	Peak power hours needed	Battery Life without Peak Power in Days
Solar Panel	1.17Amps	5.40	
BP24 Battery Rating			3.80
60 Amp-hour battery Rating			9.49

Values are based on 6.32 Amp Hour/Day required
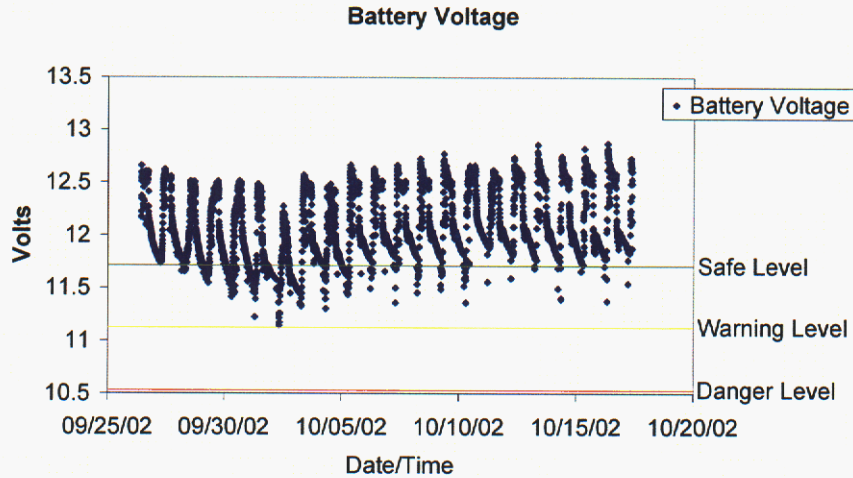
Battery Voltage

Figure 25. Battery voltage levels as measured during testing period using 24 Amp-hour battery.
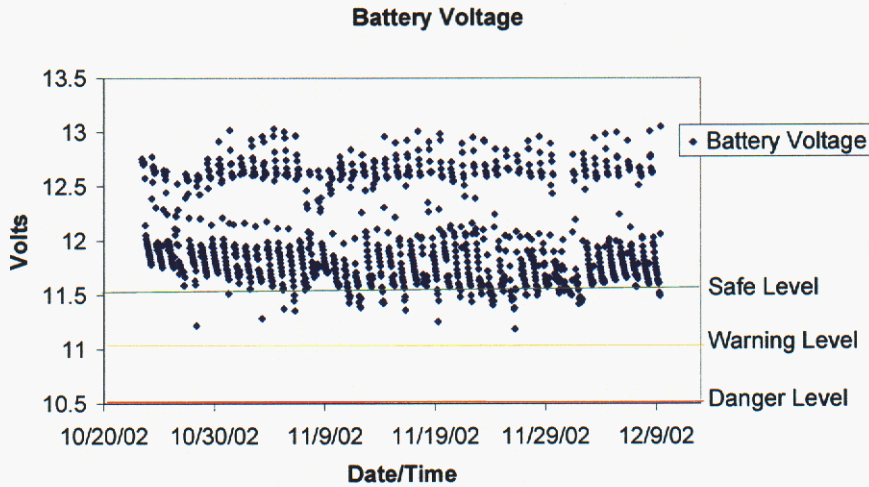
Figure 26. Battery voltage levels as measured during ambient period using 60 Amp-hour battery.

3.2.3 Chemiresistor Test (May–June, 2003)

In this first sandbox test, the chemiresistor array, C4, was used (see Figure 2). It contained the following polymers: polyepichlorohydrin (PECH), poly(N-vinyl pyrrolidone) (PNVP), polyisobutylene (PIB), and poly(ethylene-vinyl acetate) copolymer (PEVA). The univariate calibration curves for this sensor array are presented in Appendix C. The primary purpose of this test was to determine the engineering requirements and feasibility of operating and monitoring the chemiresistor by remote means.

Table 11 provides a summary of the activities performed during this test. Three major activities were performed: (1) a nearly two-week period of ambient background data collection to identify trends in drift and temperature/humidity dependence; (2) emplacement of TCE; and (3) an air-injection period to purge the sandbox of TCE. Note that the emplacement of TCE was performed twice because the initial emplacement of 30 ml was not sufficient to saturate the entire sandbox with TCE vapors.

Table 11. Summary of activities for chemiresistor test performed from May–June, 2002.

Date	Time	Activity
20-May-02	12:00	• Data taken in lab
22-May-02	9:00	• Sandbox setup, background data taken. • Sensor assembly in 25 cm well. • Start data collection

39

Date	Time	Activity
5-Jun-02	15:25 15:30	• 30 ml TCE added to wick in jar. • Wick is placed in center well. • Data collection
6-Jun-02	15:09	• Repair Res #5 RTD Temp sensor
10-Jun-02	9:07 9:16	• 200 ml TCE added to new larger wick in jar. • Wick is placed in center well. • Sensor assembly in 25 cm well. • Data collection
17-Jun-02	8:15 8:35 8:40	• At HSC • Download data • Remove top covering • Data collection
19-Jun-02	13:48	• Start air purging • psi:10 flow: 0.033 m^3/L
20-Jun-02	8:00 8:25	• Stop air purge - tank was empty • Vol: 6.816 m^3 • Remove sensor

The ambient background data-collection period was used to generate temperature-calibration curves for the individual polymers (see Section 3.1.2.3 for details). Although the sandbox was insulated, diurnal temperature fluctuations of 1-2 °C still occurred inside the sandbox. The temperature-corrected resistances provided more stable responses in the presence of these diurnal fluctuations. Corrections to fluctuations in water vapor pressure (i.e., relative humidity and temperature) were also investigated, but these variations were ultimately neglected in the univariate analyses. The univariate calibration curves (see Appendix C) were applied to measured chemiresistor resistances to generate plots of TCE vapor concentrations measured by the chemiresistor array. Figure 27 shows a plot of the measured TCE vapor concentrations for all four polymers. The responses are all within an order of magnitude of each other, and the impact of the emplacement of the TCE (30 ml on June 5 and 200 ml on June 10) is quite clear. The response of the PECH polymer is erratic (oscillatory), even with the temperature correction, which is atypical (the PECH polymer generally has a very stable response). After the initial increase in measured concentrations following TCE emplacement, the results show that the measured concentrations decrease gradually. This is a result of several small openings along the seams of the sandbox where the bottom panel and side panels of the sandbox joined together. These openings allowed the TCE to diffuse to the surroundings outside the sandbox, and barometric pressure fluctuations may have induced slight advective flow patterns as well. As a result, the TCE vapor concentrations did not increase to saturated values, and they decreased gradually after reaching a peak value shortly after emplacement of the TCE.

Although time did not permit the use of multivariate analysis of the data during the field test, we performed a multivariate partial-least squares analysis after the test was performed. Figure 28 shows the results of the multivariate analysis, which provides results that are similar to the average of the univariate results. Ongoing studies using Statistica® are providing multivariate

regression and factor analyses that can be easily programmed in the Campbell data loggers for real-time analyses of these sensors.
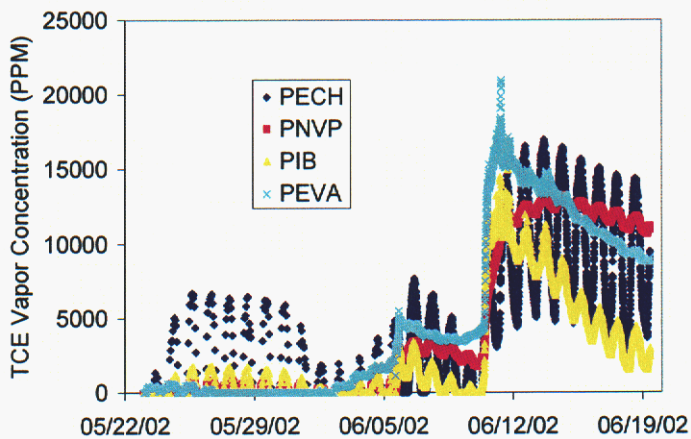
Figure 27. Measured TCE vapor concentrations using chemiresistor array (C4) and univariate calibrations and temperature corrections.
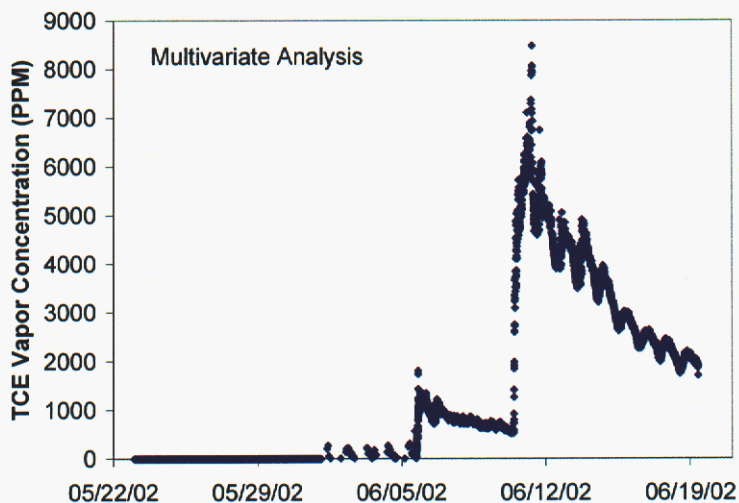
Figure 28. Measured TCE vapor concentrations using chemiresistor array (C4) and multivariate partial-least-squares data analysis.

During this test, the data were logged once and hour and posted to a web site, which provided a continuous, remote-monitoring capability. Figure 29 shows a couple screen images of the web posting of the chemiresistor-test data.
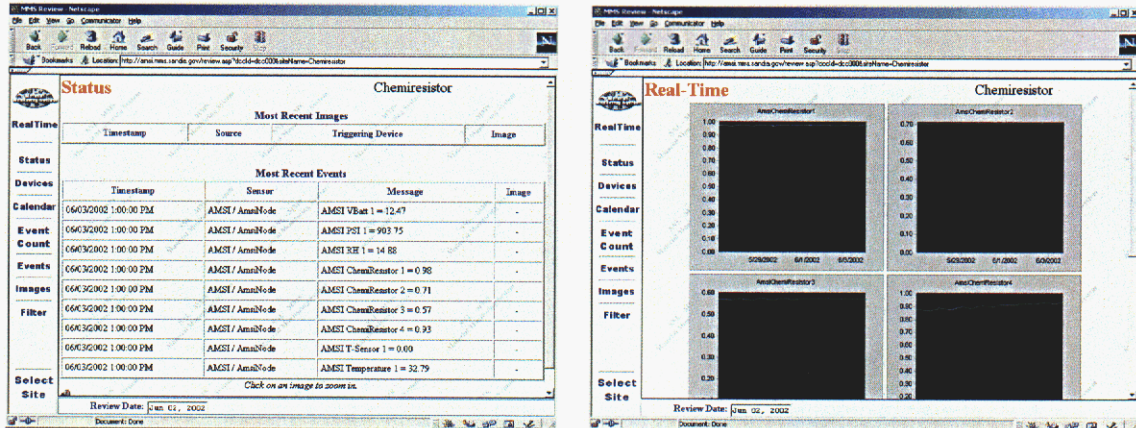
Figure 29. Screen images of real-time web posting of chemiresistor-test data.

3.2.4 Chemiresistor and SAW Test (September–December, 2002)

Following the chemiresistor test conducted in May/June, a similar test was conducted from September to December to test the SAW sensor (see Section 2.2) side-by-side with the chemiresistor. For this test, SAW sensor P9 was evaluated with chemiresistor E2. The same apparatus and experimental approach was used. The only difference was that the SAW sensor probe was emplaced alongside the chemiresistor probe (see Figure 30). A summary of activities performed during this test is provided in Table 12.
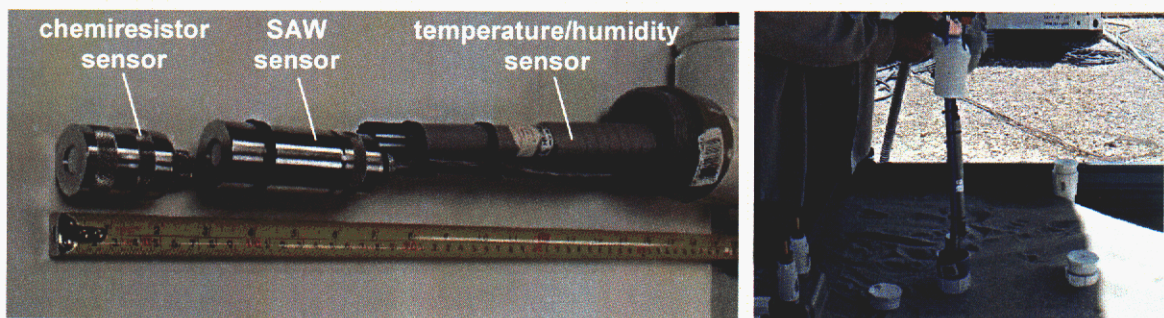
Figure 30. Sensors deployed during side-by-side test of chemiresistor and SAW sensors.

Table 12. Summary of activities for chemiresistor/SAW test performed from September-December, 2002.

Date	Time	Activity
9/23/02	10:00	• Sensors connected to data logger in lab (190)
9/26/02	9:00	• Sensors installed in sandbox (25 cm away from contaminant well)
	10:00	• Background data collected started
9/30/02	14:50	• 200 ml TCE added to wick
	15:00	• Wick placed in center well
		• Data collection continued
10/14/02	10:30	• Started venting with compressed air
		• Flow was set at ~5 psi, 0.033 m^3/min; it ran for about 3.5 hrs with a total of 6.84 m^3
10/23/02-12/09/02		• Long-term ambient monitoring period

After the sensors were installed in the sandbox, the background ambient data-collection period was used to evaluate the dependence of the SAW and chemiresistor sensors to environmental parameter fluctuations (e.g., temperature, humidity). Figure 31 and Figure 32 show the response of the chemiresistor and SAW sensors (using the PIB polymer, which was common to both sensors) to variations in temperature (other polymers behaved similarly for the respective devices). The chemiresistor exhibited a linear response to temperature, but the SAW sensor exhibited some spurious behavior. These curves were used to correct for temperature variations during the test.
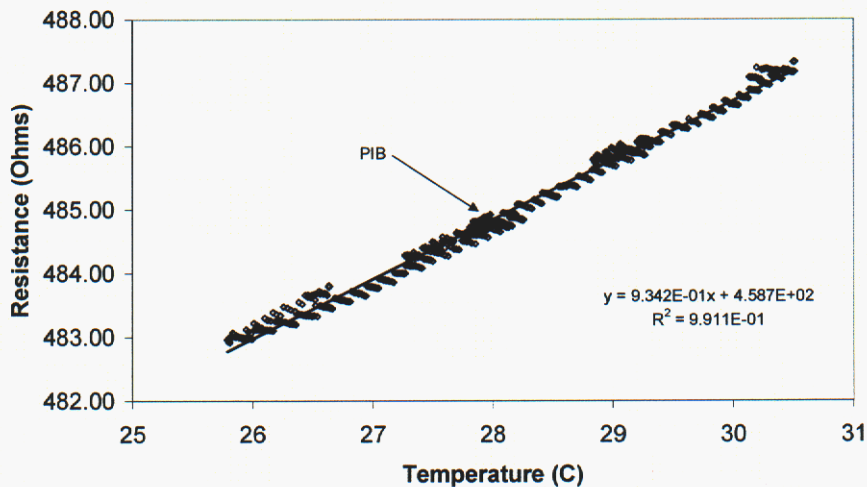
Figure 31. Chemiresistor PIB response as a function of temperature.
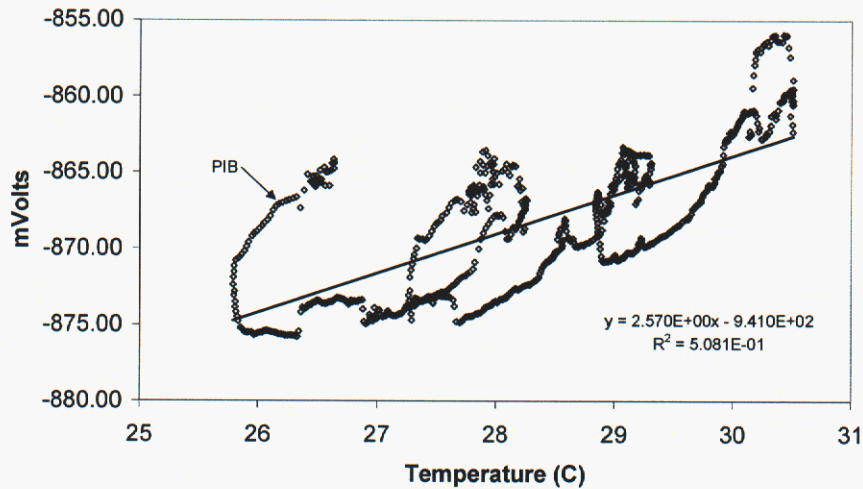
Figure 32. SAW PIB response as a function of temperature

Figure 33 shows the measured TCE vapor concentrations from the chemiresistor array using the univariate calibration curves (see Section 2.3) and temperature corrections. Noticeable responses can be seen from all four of the polymers when the TCE was emplaced on 9/30/02. The univariate responses from PECH, PNVP, and PIB all reached about 15% of the TCE saturated vapor concentration (~15,000 ppm) while PEVA reached ~60% of saturated values (60,000 ppm). The extreme difference between PEVA and the other polymers is likely caused by calibration error of the PEVA polymer. The previous sandbox experiment yielded maximum TCE vapor concentrations that were consistent with the PNVP, PIB, and PECH polymers shown in Figure 33. Figure 33 also shows a noticeable impact from the venting period. The response of all four polymers decreases due to the purging of dry air. We speculate that the air decreased the relative humidity in the sandbox and also removed any residual TCE.

Figure 34 shows the measured TCE vapor concentrations from the SAW sensor using the univariate calibration curves (see Section 2.3) and temperature corrections. The responses from the three SAW polymers (PVTD1, PVTD2, and PIB) are not consistent, either in magnitude or with time. In addition, the ventilation of dry air did not seem to impact the response of the SAW sensor. Only PVTD2 appears to provide a response that is similar to the chemiresistor (and consistent to the previous sandbox experiment). PVTD1 also provides a rapid response to the initial TCE emplacement on 9/30/02, but then it rises rapidly again after 10/1/02. The response of the PIB polymer in the SAW sensor displayed a very slow increase followed by a gradual decrease in estimated concentration, but we believe that this is more correlated to the change in ambient temperature.
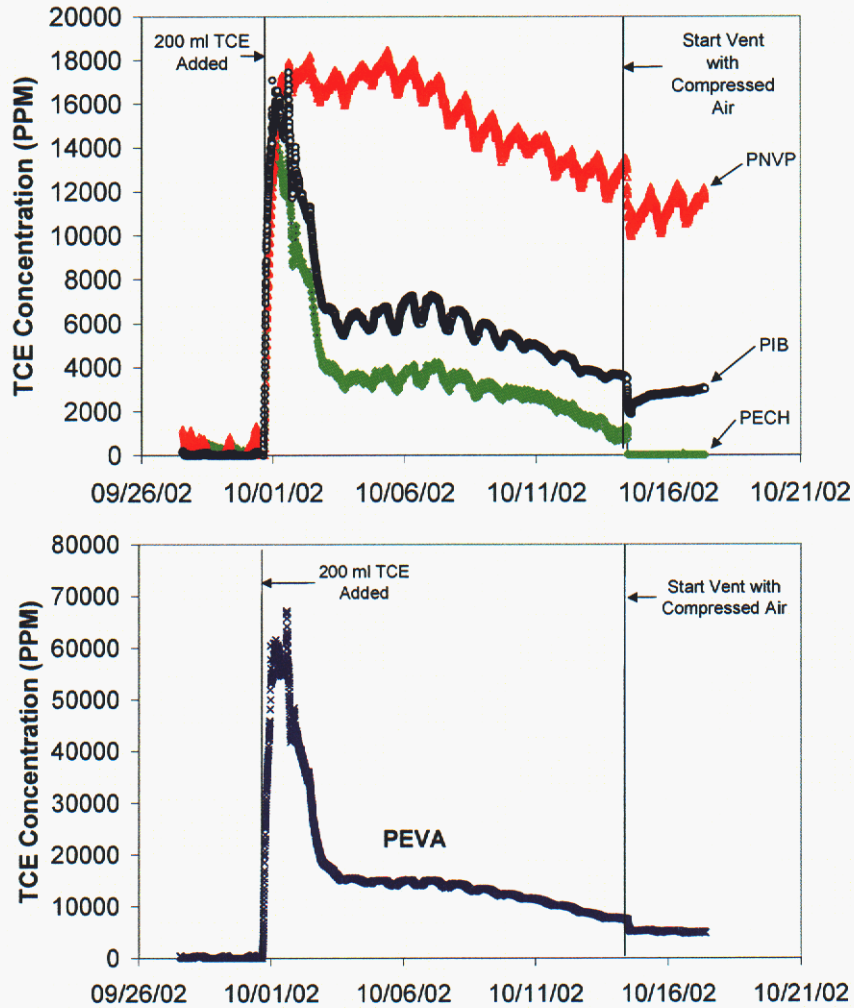
Figure 33. TCE vapor concentrations measured by the chemiresistor array (E2). Note: results from the PEVA polymer are shown on a separate (bottom) plot because of the larger readings.

Following the ventilation, a long-term ambient period (October–December) commenced to evaluate both the response of the sensors and the capability of the remote data-logging instrumentation to collect data for longer periods. In addition, the Campbell data-logging program was modified to output TCE concentrations directly from the measured signal responses (see Appendix D). The univariate calibration curves and temperature corrections were included in the program.
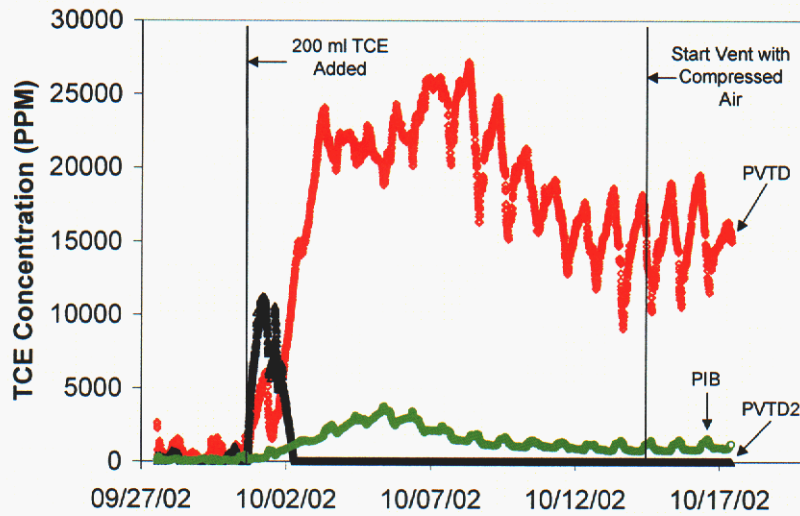
Figure 34. Measured TCE vapor concentrations from the SAW (P9) sensor.

Figure 35 shows the output of the chemiresistor sensor array during the long-term ambient monitoring period. Results show that the output from all of the polymers except for PNVP were quite stable. The PNVP exhibited significant drift, probably due to the absorption of water vapor (PNVP is a polar polymer). In addition, all of the polymers reported measuring a finite amount of TCE vapor concentration, when, in fact, no TCE should have been present during this period. A likely reason for the discrepancy is that the baseline resistances used in the program were determined at the beginning of the test (9/27/02-9/30/02). Exposure to TCE may have caused some hysteresis in the polymers such that they did not revert back to their baseline resistances. This suggests the need for a periodic re-baselining of the chemiresistors (reassigning the baseline resistance when no chemical is present).

Figure 36 shows the results of the SAW sensor during the long-term ambient monitoring period. All three polymers exhibited unstable responses during this time, even with temperature correction. In particular, the responses from the two PVTD polymers varied significantly, with no systematic trend. This is mostly likely due to the variations in ambient temperature over the 48-day period (16.8°C to 30.5°C); even though temperature corrections were applied, the variation in the SAW output did not appear to be as well correlated to the temperature variations as the chemiresistor output. The measured SAW concentrations all showed finite values of TCE during this ambient monitoring period, indicating the need to re-baseline the sensor during long test periods.
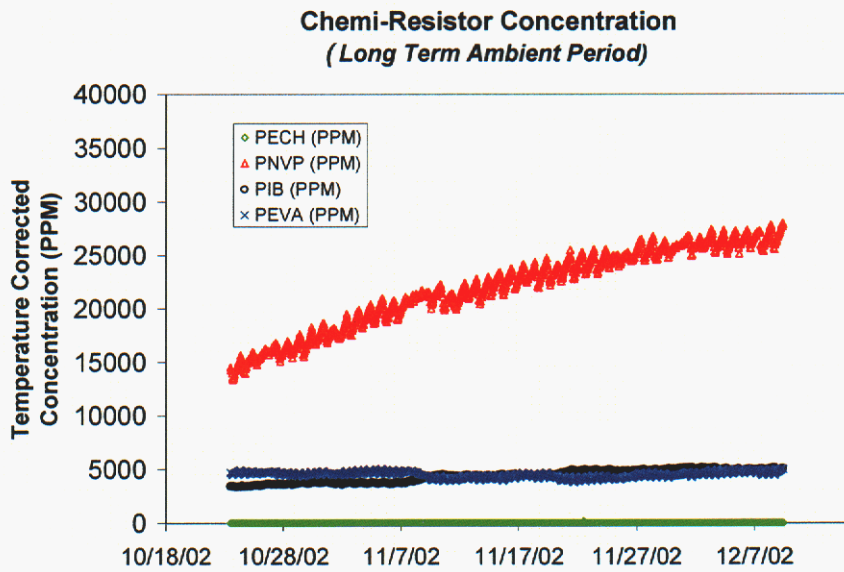
Figure 35. Measured TCE vapor concentration from the chemiresistor array during the long-term ambient monitoring period.
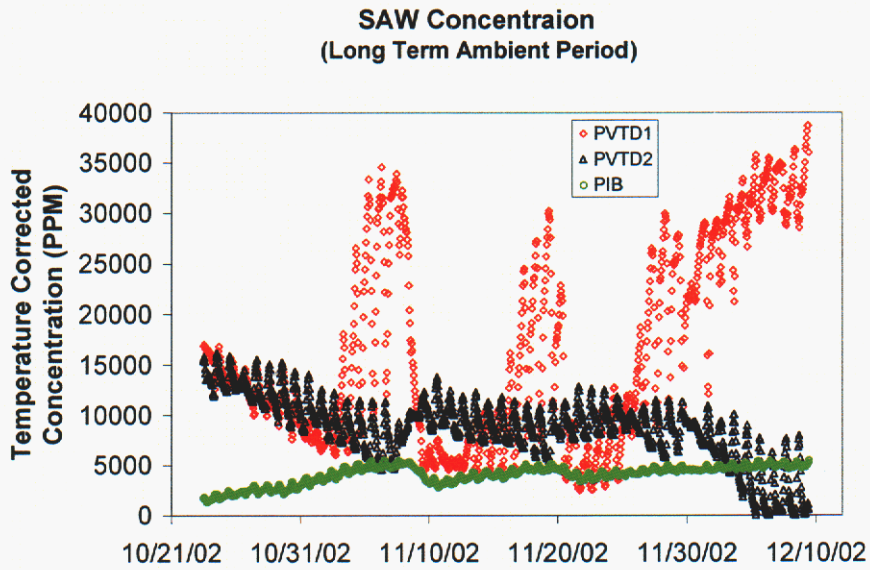
Figure 36. Measured TCE vapor concentration from the SAW sensor array during the long-term ambient monitoring period.

4.   Discussion

4.1   Dependence of Sensor Response to Environmental Variables

A significant finding of these field tests is that both the chemiresistor and SAW sensors responded to fluctuations in environmental variables (e.g., temperature, humidity). Figure 37 shows plots of barometric pressure, temperature, and relative humidity during the long-term ambient monitoring period of the sandbox test (October-December, 2002). Diurnal fluctuations as well as seasonal trends are evident in the plots. Although we attempted to correct for temperature variations during the field tests, we did not consider the impact of variations in relative humidity (water vapor pressure) or atmospheric pressures. The purpose of this section is to evaluate the relative importance of each of these environmental parameters on the measured response of the chemiresistor and SAW sensors. It is important to note, however, that subsurface environmental conditions (temperature, humidity) are typically very constant.
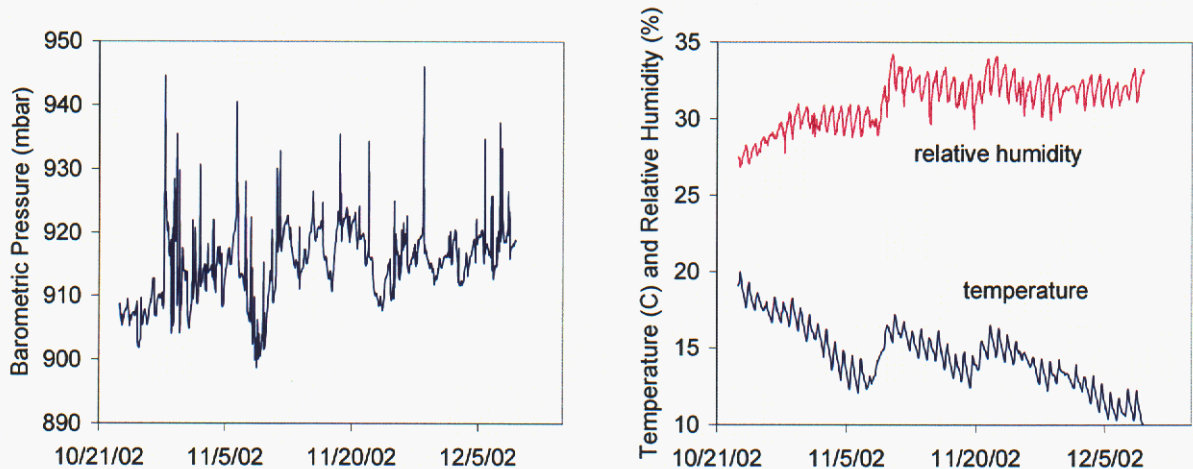
Figure 37. Environmental variable fluctuations during the long-term ambient monitoring period (October-December, 2002).

Analyses can be performed to determine the sensitivity of the dependent variables (e.g., chemiresistor resistances and SAW voltages) to the independent variables (e.g., temperature, water vapor pressure). A stepwise linear regression is a modified version of multiple regression that selectively adds input parameters (independent variables) to the regression model in successive steps. The stepwise process continues until no more variables with a significant effect on the dependent variable are found. The order of parameter selection for incorporation into the regression model gives an indication of their relative importance. The change in the coefficient of determination (ΔR^2) for a given step indicates the fraction of the variance in the model output explained by the input parameter added in that step.

Correlations between the sensor responses and the environmental variables were determined using Statistica (a commercial software package), which performed the stepwise linear-regression analysis. Several independent variables were chosen (temperature, water vapor pressure, atmospheric pressure, and battery voltage) and ranked according to their values. The dependent variables (chemiresistor resistances and SAW voltages) were also ranked, and the stepwise linear regression was performed between each of the dependent variables and the independent variables. Table 13 and Table 14 show the results of the regression analysis for both the chemiresistor and SAW sensors. Variables that are listed were found by Statistica to be statistically significant in creating variance in the sensor output. The semi-partial correlation coefficient also indicates the relative importance of the independent variables, but they also indicate whether the correlation is positive or negative.

Table 13. Stepwise linear regression analysis of chemiresistor responses (E2) to several input variables.

Step	Variable Name	R^2	ΔR^2	Semi-Partial Correlation
Chemiresistor PECH Polymer				
1	Temperature	0.975389	0.975389	0.189615
2	Elapsed Time	0.984811	0.009422	0.062532
3	Water Vapor Pressure	0.985887	0.001075	0.045623
4	Battery Voltage	0.987272	0.001385	0.038953
5	Barometric Pressure	0.987597	0.000325	-0.018036
Chemiresistor PNVP Polymer				
1	Elapsed Time	0.539798	0.539798	0.645432
2	Water Vapor Pressure	0.871310	0.331512	0.225512
3	Barometric Pressure	0.872208	0.000897	-0.033859
Chemiresistor PIB Polymer				
1	Water Vapor Pressure	0.379232	0.379232	0.233814
2	Elapsed Time	0.824350	0.445118	0.547782
3	Temperature	0.841558	0.017208	0.079642
4	Barometric Pressure	0.845710	0.004152	-0.071248
5	Battery Voltage	0.850141	0.004432	0.066572
Chemiresistor PEVA Polymer				
1	Temperature	0.907071	0.907071	0.134180
2	Elapsed Time	0.980733	0.073662	-0.239459
3	Water Vapor Pressure	0.980802	0.000069	0.008325

Table 13 shows that temperature was a significant contributor to the variance for both the PECH and PEVA polymers. Larger temperatures caused notable increases in resistances for these polymers. The elapsed time was also found to be positively correlated to all four chemiresistor polymers. This indicates that drift can be an important factor. Drift can be included in the

models, or the sensors can be re-baselined periodically. Water vapor pressure was also found to be positively correlated to the output, particularly with the PNVP and PIB polymers. The barometric pressure was generally inversely correlated to the chemiresistor output (higher pressures may have compressed the polymer, which in turn compacted the carbon particles and lowered the resistances), but the impact was found to be small. The impact of fluctuations in the battery voltage were also found to be small on the chemiresistor output.

Table 14 shows the stepwise linear regression results for the SAW sensor. In general, the SAW sensor experienced variations in response that were not as well correlated to the input variables. The coefficients of determination (R^2) for the SAW regression are generally smaller. Temperature and water-vapor pressure appear to be the most significant parameters that cause variance in the SAW response. Interestingly, the battery voltage also appears positively correlated to the response as well.

Table 14. Stepwise linear regression analysis of SAW (P9) responses to several input variables.

Step	Variable Name	R^2	ΔR^2	Semi-Partial Correlation
SAW PVTD1 Polymer				
1	Water Vapor Pressure	0.441656	0.441656	0.041782
2	Elapsed Time	0.486609	0.044953	0.275363
3	Temperature	0.524693	0.038084	0.194956
4	Barometric Pressure	0.537501	0.012808	0.108724
SAW PVTD2 Polymer				
1	Temperature	0.895251	0.895251	0.308806
2	Battery Voltage	0.924841	0.029590	0.131383
3	Water Vapor Pressure	0.930437	0.005596	-0.110808
4	Elapsed Time	0.944362	0.013925	0.118978
5	Barometric Pressure	0.945691	0.001329	-0.036455
SAW PIB Polymer				
1	Water Vapor Pressure	0.581731	0.581731	-0.086602
2	Battery Voltage	0.683787	0.102056	0.343002
3	Temperature	0.697090	0.013303	-0.126501
4	Elapsed Time	0.704180	0.007090	-0.084909

Statistical software packages such as Statistica® can be used to incorporate these input variables into multivariate predictions of chemical concentration. Interferences, fluctuating environmental variables, and even drift can all be accounted for in the model. Efforts are ongoing to developed these multivariate models.

4.2   Use of Preconcentrator to Increase Sensitivity

The theoretical detection limit of the chemiresistor is generally ~0.1-1% of the saturated vapor pressure (depending on noise and other interferences). For m-xylene, this corresponds to about 1 ppm in the aqueous phase, which is less than the maximum concentration limit (MCL) set forth by the EPA of 10 ppm in the aqueous phase. However, as indicated in Section 2.5, the theoretical detection limits of both the chemiresistor and SAW to TCE is on the order of 10-100 ppmv in the gas phase (or ~100-1000 ppb in the aqueous phase). Field tests showed that fluctuations in environmental variables and drift can increase the detection limits to above 1000 ppmv in the gas phase (~10 ppm in the aqueous phase), which is much greater than the MCL for TCE (5 ppb). As a result, although stakeholders have expressed interest in using these in-situ sensors, they are concerned about the sensitivity of the device.

A thin-film preconcentrator has been developed at Sandia to increase the sensitivity of chemiresistor and surface-acoustic-wave sensors. The thin-film preconcentrator acts as a micro-hotplate that accumulates analytes on a sorbent deposited on the thin film. After a period of exposure, the preconcentrator is quickly heated to several hundred degrees Celsius to desorb the analyte and expose the nearby sensor to a high-concentration pulse of analyte. As part of the AMSI work in FY02, we designed and fabricated an assembly that would allow the preconcentrator to be integrated with the chemiresistor sensor inside the existing waterproof housing (see Figure 38). Preliminary laboratory tests (conducted under Sandia's LDRD program) have shown that the integrated assembly is functional, and use of the preconcentrator can increase detection limits by up to two orders of magnitude. In addition, because the preconcentration involves a short-term pulsed heating process, issues such as long-term drift of the sensors are not as problematic as when the sensors are operated in a passive mode.
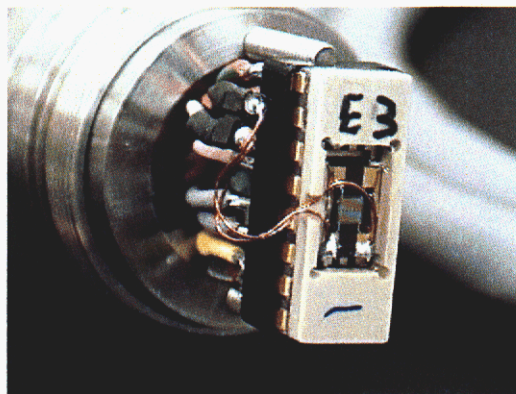
Figure 38. Preconcentrator and chemiresistor assembly integrated into waterproof probe.

4.3   Use of Temperature Control to Improve Stability

The repeatability and stability of the chemiresistor and SAW was impacted by fluctuating environmental temperatures and humidities. The 100% relative humidity environments in the 55-gallon-drum test were conducive to condensation that may have caused a continual sorption

(creep) in the polymers that contributed to long-term drift. We propose that maintaining the local temperature of the sensor above the ambient may help to prevent condensation and stabilize the sensor. This can be accomplished by using heating elements and a temperature sensor already on-board the sensor chip (see Figure 2). The temperature can be maintained in several ways:

1. Use automated temperature-control algorithm programmed in the data logger to apply a voltage to the heating element whenever the temperature of the chip (as measured by the on-board RTD) drops below a certain value.

2. Apply a constant voltage that maintains an approximate temperature based on the ambient temperature.

3. Implement an external circuit that applies variable voltage to the heating element based on the temperature difference between the RTD and the desired temperature.

The first option has been attempted with some success. The application of a fixed voltage to the heating elements on a periodic basis, however, yields significant oscillations about the desired temperature. The second option has also been attempted, and this yields the most stable temperatures. However, the resulting chip temperature can still vary if the ambient temperature is fluctuating. The third option is currently under investigation as part of Sandia's LDRD program.

5. Summary and Recommendations

Several field tests have been conducted at the Nevada Test Site to evaluate the feasibility of using chemiresistor and SAW sensors to monitor volatile organic contaminants in subsurface environments. The combination of customized packaging for the sensors and commercial data acquisition systems allowed the chemiresistor and SAW sensors to be operated remotely and continuously during the tests. Important results, findings, and recommendations from this work are summarized below:

- The SAW performance was improved through the use of a running average, which reduced the noise of the signal.

- The performance of the sensors in the field were impacted by diurnal and seasonal temperature/humidity fluctuations. Correction factors were applied to reduce the impacts of these effects.

- Although univariate temperature corrections appeared to aid in the stability of the results, in-situ calibration (or re-baselining) is desirable to alleviate the impacts of drift or fluctuations in ambient conditions. Long-term results showed that these factors can cause significant variability in the output, especially in the SAW devices. Multivariate regression methods (e.g., using Statistica®) that account for drift and multiple inputs and interferences (temperature, water-vapor pressure, etc.) should be incorporated.

- The data acquisition for the chemiresistor and SAW sensor were accomplished using a Campbell Scientific data logger powered by a 60 amp-hour battery and 20-Watt solar panel. A cell-phone modem was used to transmit the data wireless from the site to a computer where the data was processed and uploaded to the web.

- Results from the tests indicated that the chemiresistor sensor was more stable and more responsive to the TCE exposures than the SAW sensor.

6. References

Abraham, M.H., J. Andonian-Haftvan, G. Whiting, A. Leo, R.W. Taft, 1994, Hydrogen-Bonding .34. The Factors that Influence the Solubility Of Gases And Vapors In Water At 298-K, and a New Method For Its Determination, J. Chem. Soc., Perkins Trans. 2, 1777-1791.

Campbell Scientific, Inc., CR23X Micrologger® Operator's Manual, Copyright© 1986-2002 Revised 03/00, CR23X Micrologger Overview Specifications, OV-23, Logan, Utah

Campbell Scientific, Inc., LoggerNet Instruction Manual, Copyright© 1999-2002 Revised 8/02, Version 2.1, Logan, Utah

Campbell Scientific, Inc., MSC() Solar Panels Instruction Manual, Copyright© 1987-2001 Revised 10/01, 2. Specification, Logan, Utah

Campbell Scientific, Inc., COM100 Cellular Phone Package Instruction Manual, Copyright© 1987-2001, Logan, Utah

Grate, J. W., S.J. Patrash, and M.H. Abraham, 1995, Method for Estimating Polymer-Coated Acoustic Wave Vapor Sensor Responses, Anal. Chem., 67(13), 2162-2169.

Ho, C.K., and R.C. Hughes, 2002, In-Situ Chemiresistor Sensor Package for Real-Time Detection of Volatile Organic Compounds in Soil and Groundwater, 2002, Sensors, 2, 23-34.

Hughes, R.C.; Casalnuovo, S.A.; Wessendorf, K.O.; Savignon, D.J.; Hietala, S; Patel, S.V.; and Heller, E.J., 2000, Integrated Chemiresistor Array for Small Sensor Platforms, SPIE Proceedings Paper 4038-62, p. 519, AeroSense 2000, April 24-28, 2000, Orlando, Florida.

Omega Engineering Inc., PX215 Pressure Transducers M2165/0395 Common Specification For All Units, Copyright© 1995, Stamford, Connecticut

Omega Engineering Inc., HX94 SS RH Probe User's Guide, Copyright© 1996, Stamford, Connecticut

Gossett, J.M., 1987, Measurement of Henry's Law Constants for C_1 and C_2 Chlorinated Hydrocarbons, Environ. Sci. Technol., 21, 202-208.

Potyrailo, R.A., T.M. Sivavec, and A.A. Bracco, 2001, Field Evaluation of Acoustic Wave Chemical Sensors for Monitoring of Solvents in Groundwater, GE Research & Development Center Report 2000CRD092, April 2001.

7. Appendices

Appendix A: Calibration of Chemiresistor and SAW Sensors under Different Environmental Conditions

Most of the sensors that were used at the NTS field tests were calibrated to TCE under constant temperature and humidity (dry) conditions. Ideally, the chemiresistor and SAW sensors should be calibrated to TCE under different environmental conditions. These rigorous calibrations are needed to provide accurate measurements of TCE concentration when environmental variables are fluctuating. Therefore, additional calibrations were performed during and after the field test, but these were not implemented in Sections 3.2.4 due to time constraints.

The SAW "UNK" and chemiresistor E19 were calibrated to different environmental conditions. The sensors were calibrated to determine (1) response to temperature alone, (2) response to different concentrations of TCE at different temperatures, (3) response to different levels of water vapor, and (3) response to different levels of water vapor in the presence of different concentrations of TCE.

Appendix A.1: Temperature Calibrations

The two sensors (SAW UNK and chemiresistor E19) were connected to the Agilent 34970A and placed in separate 6-inch steel tubes located in an oven. Connected to the steel tubes was a 60 ft length of copper tubing that split into two lines to ensure that both sensors received approximately the same flow. The entire length of copper tubing was located in the oven to ensure that the temperature of the dry air passing the sensors was the same temperature as the oven. The oven was then turned on to 40 °C and the temperature of the sensors was monitored using the temperature-calibrated RTD on the chemiresistor. Once the RTD read a stable temperature, the oven was turned off and allowed to cool slowly while dry air flowed over the sensors. Once the temperature of the oven reached 23 °C (room temperature) the experiment was stopped and the dry air was turned off. Then, the data was exported from the Agilent. The temperature was plotted against the raw readouts of the polymers and Microsoft Excel was used to calculate a linear regression curve to fit each polymer. Figure 39 and Figure 40 show plots of the cooling period for the chemiresistor E19 and SAW UNK, respectively, and the results of the linear regressions for the chemiresistor E19 and SAW UNK are shown in Table 15.
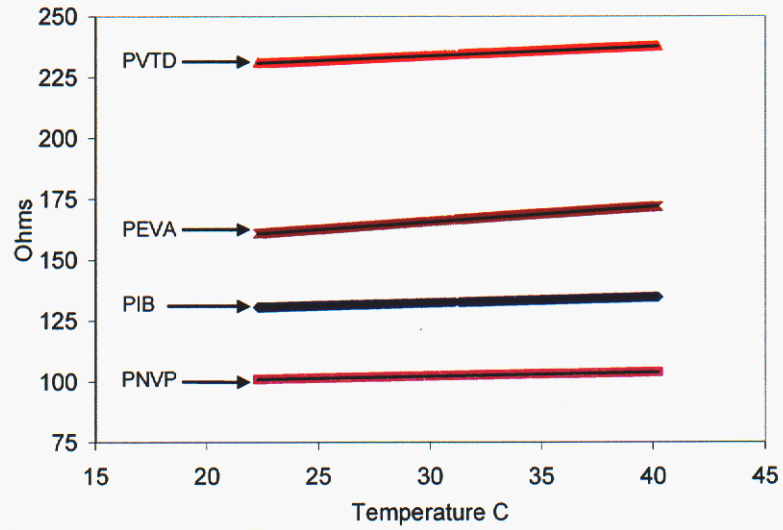
Figure 39. Temperature dependence of chemiresistor E19.
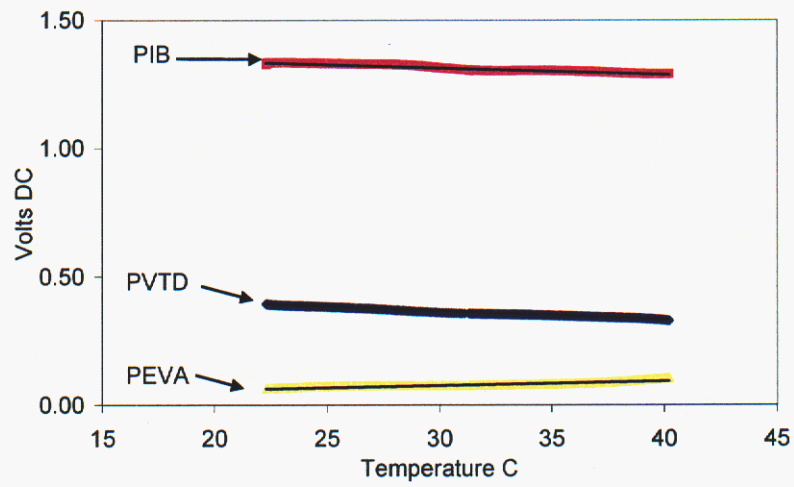
Figure 40. Temperature dependence of SAW UNK

Table 15. Temperature calibrations for SAW UNK and chemiresistor E19.

	Polymer	Regression Type	Regression	R^2
Chemiresistor E19	PIB	Linear	y = 0.2279x + 125.53	1.00
	PNVP	Linear	y = 0.167x + 97.305	1.00
	PVTD	Linear	y = 0.3871x + 222.32	0.999
	PEVA	Linear	y = 0.624x + 147.02	0.999
SAW UNK	PEVA	Linear	y = 0.0017x + 0.025	0.911
	PIB	Linear	y = -0.0026x + 1.3917	0.965
	PVTD	Linear	y = -0.0034x + 0.4675	0.993

y = Raw Resistance for chemiresistor and Raw Voltage for SAW
x = Temperature in degrees Celsius

Appendix A.2: TCE Calibrations at Different Temperatures

First, the chemiresistor E19 and the SAW UNK were calibrated for different TCE concentrations at room temperature, 23 °C. A similar apparatus to the one in Figure 7 was used. Dry air flowed across the sensor until they reached a stable baseline. Then, TCE was added to the system. After the sensors stabilized in the new environment, dry air was added. This method of adding a known concentration of TCE followed by the addition of dry air was followed for 50-ppm TCE, 500-ppm TCE, 1000-ppm TCE, and 10,000-ppm TCE at room temperature. The concentrations of TCE were verified with the M200 gas chromatograph. The same mathematical procedure found in Section 2.3 was used to calculate the $\Delta R/R_b$ values for the chemiresistor E19 and $\Delta V/V_b$ values for the SAW UNK.

Next, the SAW UNK and chemiresistor E19 were placed in separate steel tubes and placed in the oven. The effluent gas was split in two after flowing through 60-ft copper tubing. The oven was turned on to 30 °C. Then dry air was turned on to flow over the sensors. The temperatures of the sensors were allowed stabilize. The temperature calibrated RTD on the chemiresistor verified the temperature to be 30 C and once the temperature had stabilized the first concentration of TCE was added to the system. Once the sensors had stabilized in the new environment the TCE was turned off and dry air flow began once again. This method was used for 50-ppm TCE, 500-ppm TCE, 1000-ppm TCE, and 10,000-ppm. The data was then exported from the Agilent data logger and processed. The same apparatus and procedure used in the 30 °C calibration was also used for a cold-temperature calibration inside a refrigerator that was set to the minimum setting, which yielded 9 °C. Figure 41 and Figure 42 show the response chemiresistor E19 to different TCE concentrations under different temperatures.
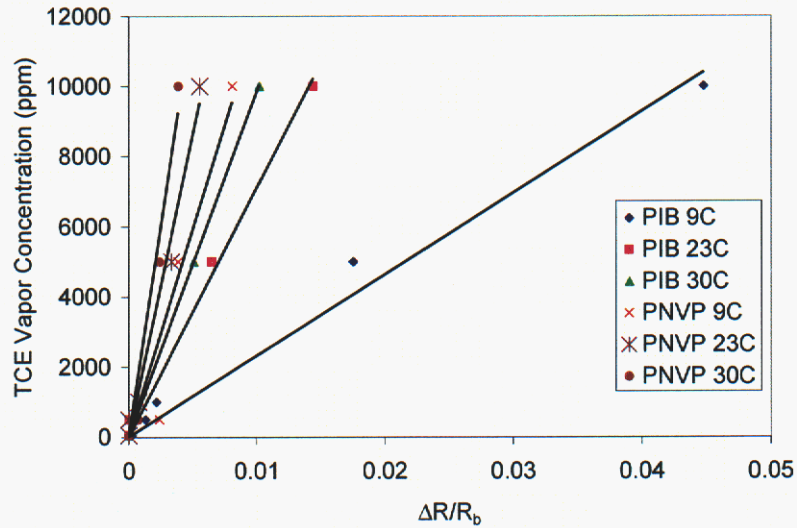
Figure 41. E19 TCE calibration of PIB and PNVP on chemiresistor E19 at different temperatures in dry conditions.
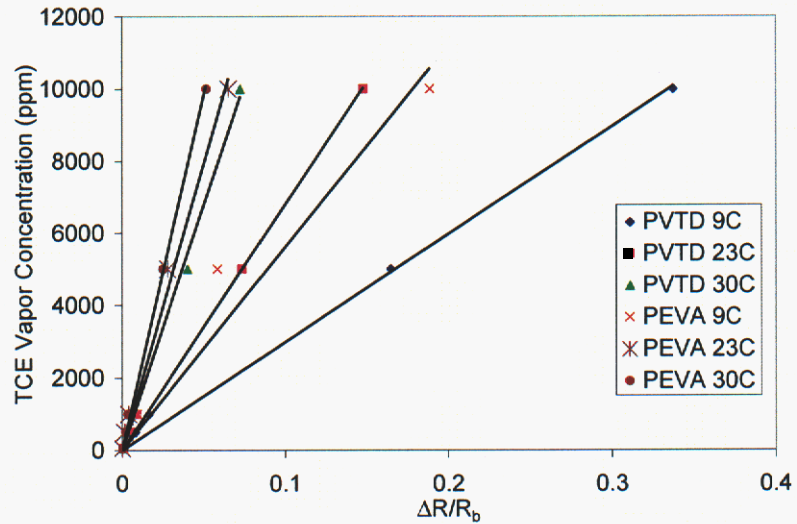
Figure 42. E19 TCE calibration of PVTD and PEVA on chemiresistor E19 at different temperatures in dry conditions.

Figure 43 shows the response of SAW UNK to different TCE concentrations under different temperature conditions. The polymer PIB was considered non-functional and was not included in the analysis of the runs. Table 16 shows the calculated linear regressions and their respective correlation coefficients for the TCE calibrations for both chemiresistor E19 and SAW UNK.
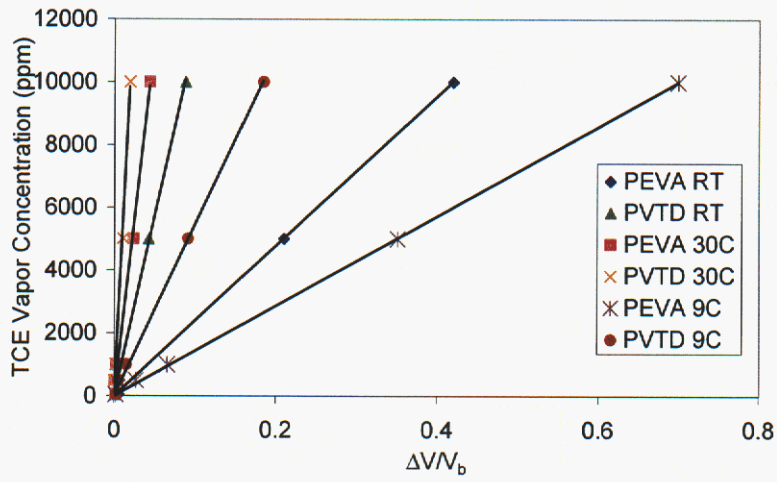
Figure 43. TCE calibration of SAW UNK at different temperatures under dry conditions.

Table 16. TCE calibration for chemiresistor E19 and SAW UNK at different temperatures.

	Polymer	Temperature	Regression Type	Regression (ppm)	R2	Regression (g/L)	R2
Chemiresistor E19	PIB	9C	Linear	$y_1 = 2.321E{+}05x$	0.982	$y_2 = 1.0483x$	0.982
		23C	Linear	$y_1 = 7.099E{+}05x$	0.991	$y_2 = 3.2066x$	0.991
		30C	Linear	$y_1 = 9.836E{+}05x$	0.999	$y_2 = 4.4428x$	0.999
	PNVP	9C	Linear	$y_1 = 1.178E{+}06x$	0.920	$y_2 = 5.3203x$	0.920
		23C	Linear	$y_1 = 1.712E{+}06x$	0.984	$y_2 = 7.7332x$	0.984
		30C	Linear	$y_1 = 2.385E{+}06x$	0.959	$y_2 = 10.772x$	0.959
	PVTD	9C	Linear	$y_1 = 2.986E{+}04x$	0.995	$y_2 = 0.1349x$	0.995
		23C	Linear	$y_1 = 6.798E{+}04x$	0.997	$y_2 = 0.3071x$	0.997
		30C	Linear	$y_1 = 1.354E{+}05x$	0.995	$y_2 = 0.8841x$	0.998
	PEVA	9C	Linear	$y_1 = 5.613E{+}04x$	0.950	$y_2 = 0.2535x$	0.950
		23C	Linear	$y_1 = 1.579E{+}05x$	0.991	$y_2 = 0.7131x$	0.991
		30C	Linear	$y_1 = 1.957E{+}05x$	0.998	$y_2 = 0.6115x$	0.995
SAW UNK	PEVA	9C	Linear	$y_1 = 1.430E{+}04x$	1.000	$y_2 = 0.0646x$	1.000
		23C	Linear	$y_1 = 2.385E{+}04x$	0.810	$y_2 = 0.1077x$	0.810
		30C	Linear	$y_1 = 2.279E{+}05x$	0.992	$y_2 = 1.0294x$	0.992
	PVTD	9C	Linear	$y_1 = 5.447E{+}04x$	0.999	$y_2 = 0.246x$	0.999
		23C	Linear	$y_1 = 1.147E{+}05x$	0.991	$y_2 = 0.5182x$	0.991
		30C	Linear	$y_1 = 5.294E{+}05x$	0.994	$y_2 = 2.3913x$	0.994

y_1 = TCE vapor concentration (ppm)
y_2 = TCE vapor concentration (g/L)
$x = \Delta R/R_b$ for chemiresistor $\Delta V/V_b$ for SAW

58

Appendix A.3: Water-Vapor Calibrations

In this calibration, the dry air lines were split so that a controlled amount of dry air could flow through a bubbler filled with de-ionized water while the other line would contain dry air. The lines were combined prior to flow through the M200 gas chromatograph and the sensors so that the actual water vapor concentration could be varied and monitored based on the relative amount of flow through the water bubbler. The average local atmospheric pressure during the experiments was 83,430 Pa (this value was used to convert units of Pa to ppmv). Figure 44 shows the response of chemiresistor E19 to water vapor.
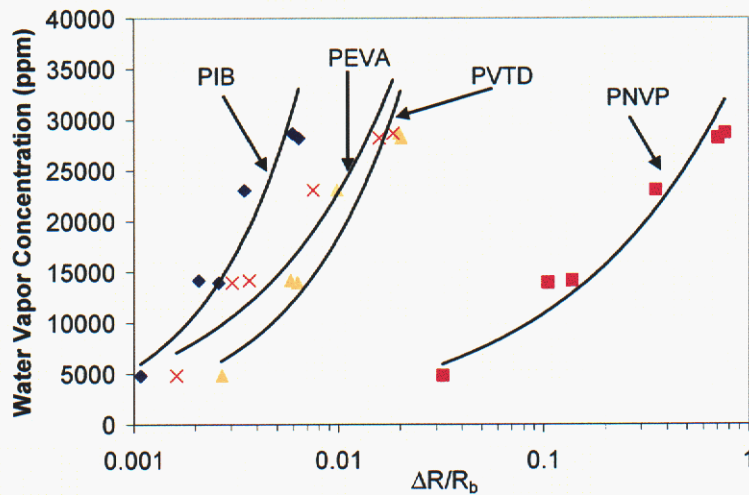
Figure 44. Chemiresistor E19 response to water vapor.

The $\Delta V/V_b$ vs. the water vapor was plotted and power functions were fit to the data of PEVA and PVTD on the SAW UNK. PIB was omitted because the voltages were erratic. The power functions had strong correlation coefficients. Figure 45 shows the response of SAW UNK to water vapor. Table 17 shows the calculated power functions with their respective correlation coefficients for chemiresistor E19 and SAW UNK.
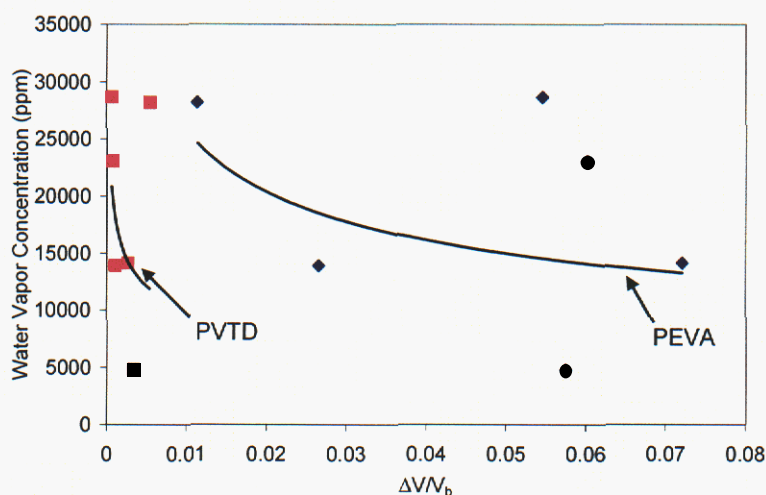
Figure 45. SAW UNK response to changes in water vapor concentrations.

Table 17. Water vapor calibration for chemiresistor E19 and SAW UNK.

	Polymer	Regression Type	Regression (ppm)	R^2	Regression (Pa)	R^2
Chemiresistor E19	PIB	Power	$y_1 = 4.246E+06x^{9.604E-01}$	0.920	$y_2 = 3.543E+05x^{9.604E-01}$	0.920
	PNVP	Power	$y_1 = 3.678E+04x^{5.301E-01}$	0.944	$y_2 = 3.068E+03x^{5.301E-01}$	0.944
	PVTD	Power	$y_1 = 8.192E+05x^{8.232E-01}$	0.908	$y_2 = 6.834E+04x^{8.232E-01}$	0.908
SAW UNK	PEVA	Power	$y_1 = 4.433E+05x^{6.436E-01}$	0.857	$y_2 = 3.698E+04x^{6.436E-01}$	0.857
	PEVA	Power	$y_1 = 5.496E+03x^{-3.349E-01}$	0.123	$y_2 = 4.585E+02x^{-3.349E-01}$	0.123
	PVTD	Power	$y_1 = 3.013E+03x^{-2.634E-01}$	0.119	$y_2 = 2.514E+02x^{-2.634E-01}$	0.119

y_1= Water Vapor (ppm)
y_2 = Water Vapor (Pa)
$x = \Delta R/R_b$ for chemiresistor $\Delta V/V_b$ for SAW

Appendix A.4: TCE Calibration at Different Water-Vapor Concentrations

The same apparatus used in the water-vapor calibrations was used to perform the calibration of the sensors to TCE at different water-vapor concentrations. Instead of diluting the water-vapor line with dry air, however, dry TCE from custom tanks was used. Varying concentrations of TCE and water vapor were achieved by varying the flow rates of TCE and air through the water bubbler. The micro-gas chromatograph was used to monitor the concentrations. Table 18 and Table 19 shows the response of chemiresistor E19 and SAW UNK to the combined exposures of TCE and water vapor.   Software such as Statistica® can be used to generate multivariate regression curves using factor analysis of the various inputs.

Table 18. Chemiresistor E19 response to TCE and water vapor calibration experiment.

Water Vapor Concentration (ppm)	TCE Vapor Concentration (ppm)	Chemiresistor E19			
		PIB	PNVP	PVTD	PEVA
		$\Delta R/R_b$	$\Delta R/R_b$	$\Delta R/R_b$	$\Delta R/R_b$
25298	164	0.004	0.296	0.012	0.008
25549	236	0.004	0.275	0.011	0.007
17583	505	0.003	0.074	0.008	0.005
9252	740	0.003	0.056	0.007	0.005
7262	795	0.003	0.054	0.007	0.005
26054	1895	0.007	0.267	0.025	0.016
25889	2562	0.008	0.226	0.027	0.020
17039	5212	0.011	0.023	0.043	0.033
9298	7469	0.014	0.032	0.058	0.055

Table 19. SAW UNK response to TCE and water vapor calibration experiment.

Water Vapor Concentration (ppm)	TCE Vapor Concentration (ppm)	SAW UNK		
		PEVA	PIB	PVTD
		$\Delta V/V_b$	$\Delta V/V_b$	$\Delta V/V_b$
25298	164	0.031	0.001	0.002
25549	236	0.017	0.001	0.003
17583	505	0.006	0.001	0.003
9252	740	0.007	0.001	0.003
7262	795	0.010	0.001	0.003
26054	1895	0.068	0.001	0.015
25889	2562	0.105	0.000	0.020
17039	5212	0.224	0.000	0.038
9298	7469	0.339	0.001	0.053

Appendix B: Programs for Campbell Scientific CR23X Data Logger

The CR23X requires a user-generated program written via the PC208(W) PC-based software program (see Appendices B.1, B.2, and B.3). This program controls the CR23X inputs and outputs.

Within the context of the following descriptions, the CR23X program in Appendix B.3 will be discussed. The referenced program in Appendix B.3 is the most complex of the programs shown. With an understanding of the program in Appendix B.3, all aspects of the remaining programs should be self-explanatory. A more detailed explanation of these programs can be found in the Campbell Scientific CR23X Micrologger© Operator's Manual. Each program consists of three primary "tables," which are described below.

Program Table 1

The execution interval for table 1 is set to 30 seconds.

Program Table 1, Instruction 1-8: Controls the enabled/disabled conditions of the cellular phone package. The CR23X controls the COM100 Cellular package through turning on/off of the control port one. The program enabled the control port at 5:00AM and disabled the control port 8:00 PM. This allows the cellular phone to be available during daytime/business hours only. During the control port enabled period the battery voltage is monitored. If the battery voltage drops below 11.5 volts the control port is disabled. If the battery voltage returns to above to above 12.2 volts the control port is enabled allowing communication. Instruction 8 Ends If time is instruction (Instruction 1)

Program Table 1, Instruction 9-61: Readings were taken as follows: RTD (Table 1, Instruction 11), Chemiresistor (Table 1, Instruction 12), and SAW (Program Table 2, Instruction 3-4).

Chemiresistor Calculations *(Program Table 1, Instruction 13-29)* were calculated per the following equations:

Conversion from voltage to resistance

1.*(Instruction 13-16):* $V_{REF} = V_{INPUT} - V_{SENS}$

2.*(Instruction 17-21):* $I_{REF} = V_{REF}/R_{REF}$

3.*(Instruction 22-25):* $-R_{SENS} = V_{SENS}/I_{REF}$

4.*(Instruction 26-29):* $(R_{SENS})(-1)$

Conversion from resistance to temperature corrected concentration

5. *(Instruction 31-34)* TempCor() = TempDiff * TempSlo()

6.(Instruction 35-38) TempCorR() = ohms_()c − TempCor()

7.(Instruction 39-42) Num() = TempCorR() − BaseLine()

8.(Instruction 43-46) DeltaRb() = Num() / BaseLine()

9.(Instruction 47-50) DeltaX() = DeltaRb()$^{ExCon()}$

10.(Instruction 51-54) (polymer)_Con = DeltaX() * Coef()

Program Table 1, Instruction 55-61): Sets the output flag high preparing the Final Data Storage location for the acceptance of the Output Array. The resolution is set high to prepare the Final Data Storage location for acceptance of a 4 byte format with 5 significant digits and a maximum possible output value of +99999. The date format is set to "1111 Year,Day,Hour/Minute,Seconds (midnight = 0000))" for processing to Final Data Storage. The final instruction is used to store each of the listed input location(s) into Final Data Storage, Hardware ID 155 (See Appendix B.5). Instruction 61 Ends If time is instruction (Instruction 9)

Program Table 1, Instruction 62-68: Starts with an, if time is 0 seconds into a 30 second interval then do the following. The hardware and environmental values are updated and placed into a 4.5 minute running average.

Program Table 2

The execution interval for table 2 is set to .4 seconds.

Program Table 2, Instruction 1-6: Starts with an if time is 59 minutes into a 60 minute interval then do the following. Begin a 60 second loop, which updates SAW values and places them into a running average. Instruction 5 Ends loop instruction. Instruction 6 Ends If time is instruction.

Program Table2, Instruction 7-11: Sets the output flag high preparing the Final Data Storage location for the acceptance of the Output Array. The resolution is set high to prepare the Final Data Storage location for acceptance of a 4 byte format with 5 significant digits and a maximum possible output value of +99999. The date format is set to "1111 Year,Day,Hour/Minute,Seconds (midnight = 0000))" for processing to Final Data Storage. The final instruction is used to store each of the listed input location(s) into Final Data Storage, Hardware ID 207 (See Appendix B.5).

Program Table 3

This table contains "subroutines" that list constants such as reference-resistor values.

Appendix B.1: Campbell CR23X Data-Logging Program for Chemiresistor(Test Program, Test Dates: 5/19/02-6/23/02)

```
;{CR23X}                          ;Date:6/5/02
;Chemiresistor Test at HSC        ;change scan rate 6/27/02
```

```
;CR23X Datalogger


*Table 1 Program
  01: 30          Execution Interval (seconds) ;

1:  If time is (P92)
 1: 1          Minutes (Seconds --) into a
 2: 60         Interval (same units as above)
 3: 41         Set Port 1 High

2:  Do (P86)
 1: 1          Call Subroutine 1

3:  Excite-Delay (SE) (P4)
 1: 1          Reps
 2: 15         5000 mV, Fast Range
 3: 9          SE Channel
 4: 1          Excite all reps w/Exchan 1
 5: 50         Delay (units 0.01 sec)
 6: 5000       mV Excitation
 7: 1          Loc [ Sen_1_mVm ]
 8: -1         Mult
 9: 0          Offset

4:  Excite-Delay (SE) (P4)
 1: 1          Reps
 2: 15         5000 mV, Fast Range
 3: 10         SE Channel
 4: 2          Excite all reps w/Exchan 2
 5: 50         Delay (units 0.01 sec)
 6: 5000       mV Excitation
 7: 2          Loc [ Sen_2_mVm ]
 8: -1         Mult
 9: 0          Offset

5:  Excite-Delay (SE) (P4)
 1: 1          Reps
 2: 15         5000 mV, Fast Range
 3: 11         SE Channel
 4: 3          Excite all reps w/Exchan 3
 5: 50         Delay (units 0.01 sec)
 6: 5000       mV Excitation
 7: 3          Loc [ Sen_3_mVm ]
 8: -1         Mult
 9: 0          Offset

6:  Excite-Delay (SE) (P4)
 1: 1          Reps
 2: 15         5000 mV, Fast Range
 3: 12         SE Channel
 4: 4          Excite all reps w/Exchan 4
 5: 50         Delay (units 0.01 sec)
 6: 5000       mV Excitation
 7: 4          Loc [ Sen_4_mVm ]
 8: -1         Mult
 9: 0          Offset

7:  Excite-Delay (SE) (P4)
 1: 1          Reps
 2: 15         5000 mV, Fast Range
 3: 8          SE Channel
 4: 1          Excite all reps w/Exchan 1
 5: 50         Delay (units 0.01 sec)
 6: 5000       mV Excitation
 7: 5          Loc [ Sen_5_mVm ]
 8: -1         Mult
 9: 0          Offset

8:  Z=X+F (P34)
 1: 1          X Loc [ Sen_1_mVm ]
 2: 5000       F
 3: 6          Z Loc [ Res_1_mVc ]

9:  Z=X+F (P34)
 1: 2          X Loc [ Sen_2_mVm ]
 2: 5000       F
 3: 7          Z Loc [ Res_2_mVc ]

10:  Z=X+F (P34)
 1: 3          X Loc [ Sen_3_mVm ]
```

```
 2: 5000       F
 3: 8          Z Loc [ Res_3_mVc ]

11:  Z=X+F (P34)
 1: 4          X Loc [ Sen_4_mVm ]
 2: 5000       F
 3: 9          Z Loc [ Res_4_mVc ]

12:  Z=X+F (P34)
 1: 5          X Loc [ Sen_5_mVm ]
 2: 5000       F
 3: 10         Z Loc [ Res_5_mVc ]

13:  Z=X/Y (P38)
 1: 6          X Loc [ Res_1_mVc ]
 2: 22         Y Loc [ Ref1_Kohm ]
 3: 11         Z Loc [ uA_1c    ]

14:  Z=X/Y (P38)
 1: 7          X Loc [ Res_2_mVc ]
 2: 23         Y Loc [ Ref2_Kohm ]
 3: 12         Z Loc [ uA_2c    ]

15:  Z=X/Y (P38)
 1: 8          X Loc [ Res_3_mVc ]
 2: 24         Y Loc [ Ref3_Kohm ]
 3: 13         Z Loc [ uA_3c    ]

16:  Z=X/Y (P38)
 1: 9          X Loc [ Res_4_mVc ]
 2: 25         Y Loc [ Ref4_Kohm ]
 3: 14         Z Loc [ uA_4c    ]

17:  Z=X/Y (P38)
 1: 10         X Loc [ Res_5_mVc ]
 2: 26         Y Loc [ Ref5_Kohm ]
 3: 15         Z Loc [ uA_5c    ]

18:  Z=X/Y (P38)
 1: 1          X Loc [ Sen_1_mVm ]
 2: 11         Y Loc [ uA_1c    ]
 3: 27         Z Loc [ negkohms1 ]

19:  Z=X/Y (P38)
 1: 2          X Loc [ Sen_2_mVm ]
 2: 12         Y Loc [ uA_2c    ]
 3: 28         Z Loc [ negkohms2 ]

20:  Z=X/Y (P38)
 1: 3          X Loc [ Sen_3_mVm ]
 2: 13         Y Loc [ uA_3c    ]
 3: 29         Z Loc [ negkohms3 ]

21:  Z=X/Y (P38)
 1: 4          X Loc [ Sen_4_mVm ]
 2: 14         Y Loc [ uA_4c    ]
 3: 30         Z Loc [ negkohms4 ]

22:  Z=X/Y (P38)
 1: 5          X Loc [ Sen_5_mVm ]
 2: 15         Y Loc [ uA_5c    ]
 3: 31         Z Loc [ negkohms5 ]

23:  Z=X*F (P37)
 1: 27         X Loc [ negkohms1 ]
 2: -1         F
 3: 16         Z Loc [ Kohms_1c  ]

24:  Z=X*F (P37)
 1: 28         X Loc [ negkohms2 ]
 2: -1         F
 3: 17         Z Loc [ Kohms_2c  ]

25:  Z=X*F (P37)
 1: 29         X Loc [ negkohms3 ]
 2: -1         F
 3: 18         Z Loc [ Kohms_3c  ]

26:  Z=X*F (P37)
 1: 30         X Loc [ negkohms4 ]
 2: -1         F
```

```
  3: 19         Z Loc [ Kohms_4c  ]

27:  Z=X*F (P37)                                   *Table 3 Subroutines
  1: 31         X Loc [ negkohms5 ]
  2: -1         F                                  1:  Beginning of Subroutine (P85)
  3: 20         Z Loc [ Kohms_5c  ]                  1: 1         Subroutine 1

28:  If time is (P92)                              2:  Z=F (P30)
  1: 0          Minutes (Seconds --) into a          1: .981      F
  2: 120        Interval (same units as above)       2: 0         Exponent of 10
  3: 10         Set Output Flag High (Flag 0)        3: 22        Z Loc [ Ref1_Kohm ]

29:  Resolution (P78)                              3:  Z=F (P30)
  1: 1          High Resolution                      1: .982      F
                                                     2: 0         Exponent of 10
30:  Real Time (P77)                                 3: 23        Z Loc [ Ref2_Kohm ]
  1: 1111       Year,Day,Hour/Minute,Seconds (midnight =
0000)                                             4:  Z=F (P30)
                                                     1: .983      F
31:  Sample (P70)                                    2: 0         Exponent of 10
  1: 5          Reps                                 3: 24        Z Loc [ Ref3_Kohm ]
  2: 1          Loc [ Sen_1_mVm ]
                                                   5:  Z=F (P30)
32:  Sample (P70)                                    1: .984      F
  1: 5          Reps                                 2: 0         Exponent of 10
  2: 16         Loc [ Kohms_1c ]                      3: 25        Z Loc [ Ref4_Kohm ]

33:  Sample (P70)                                  6:  Z=F (P30)
  1: 5          Reps                                 1: .982      F
  2: 11         Loc [ uA_1c    ]                      2: 0         Exponent of 10
                                                     3: 26        Z Loc [ Ref5_Kohm ]

                                                   7:  End (P95)
*Table 2 Program
  01: 60        Execution Interval (seconds)       End Program

1:  Batt Voltage (P10)                             -Input Locations-
  1: 32         Loc [ Bat_Vdc   ]                  1 Sen_1_mVm 1 3 1
                                                   2 Sen_2_mVm 1 3 1
2:  Panel Temperature (P17)                        3 Sen_3_mVm 1 3 1
  1: 33         Loc [ Temp_C    ]                  4 Sen_4_mVm 1 3 1
                                                   5 Sen_5_mVm 1 3 1
3:  Volt (SE) (P1)                                 6 Res_1_mVc 1 1 1
  1: 1          Reps                               7 Res_2_mVc 1 1 1
  2: 24         1000 mV, 60 Hz Reject, Slow Range  8 Res_3_mVc 1 1 1
  3: 14         SE Channel                         9 Res_4_mVc 1 1 1
  4: 34         Loc [ RHpct     ]                  10 Res_5_mVc 1 1 1
  5: .1         Mult                               11 uA_1c      1 2 1
  6: 0          Offset                             12 uA_2c      1 2 1
                                                   13 uA_3c      1 2 1
4:  Volt (SE) (P1)                                 14 uA_4c      1 2 1
  1: 1          Reps                               15 uA_5c      1 2 1
  2: 24         1000 mV, 60 Hz Reject, Slow Range  16 Kohms_1c   1 1 1
  3: 15         SE Channel                         17 Kohms_2c   1 1 1
  4: 35         Loc [ RH_Temp_C ]                  18 Kohms_3c   1 1 1
  5: .1         Mult                               19 Kohms_4c   1 1 1
  6: -40        Offset                             20 Kohms_5c   1 1 1
                                                   21 _____    0 0 0
5:  Volt (SE) (P1)                                 22 Ref1_Kohm 1 1 1
  1: 1          Reps                               23 Ref2_Kohm 1 1 1
  2: 15         5000 mV, Fast Range                24 Ref3_Kohm 1 1 1
  3: 23         SE Channel                         25 Ref4_Kohm 1 1 1
  4: 36         Loc [ BP_mbar   ]                  26 Ref5_Kohm 1 1 1
  5: .184       Mult                               27 negkohms1 1 1 1
  6: 600        Offset                             28 negkohms2 1 1 1
                                                   29 negkohms3 1 1 1
6:  If time is (P92)                               30 negkohms4 1 1 1
  1: 0          Minutes (Seconds --) into a        31 negkohms5 1 1 1
  2: 120        Interval (same units as above)     32 Bat_Vdc    1 1 1
  3: 10         Set Output Flag High (Flag 0)      33 Temp_C     1 1 1
                                                   34 RHpct      1 1 1
7:  Resolution (P78)                               35 RH_Temp_C 1 1 1
  1: 1          High Resolution                    36 BP_mbar    1 1 1
                                                   37 _____    0 0 0
8:  Real Time (P77)                                -Program Security-
  1: 1111       Year,Day,Hour/Minute,Seconds (midnight =   0000
0000)                                             0000
                                                   0000
9:  Average (P71)                                  -Mode 4-
  1: 5          Reps                               -Final Storage Area 2-
  2: 32         Loc [ Bat_Vdc   ]
```

```
0                                                        -CR10X Compile Setting-
-CR10X ID-                                               3
0                                                        -CR10X RS-232 Setting-
-CR10X Power Up-                                         -1
3
```

Appendix B.2: Campbell CR23X Data-Logging Program for Chemiresistor and SAW Measurement(Test Program, Test Dates: 9/26/02-10/23/02)

```
;{CR23X}                                                ;Call subroutine to load values from the
;NTS Test Program              *                        subroutine
;Written By: Jerome Wright &   *                         10:  Do (P86)
;            Lucas McGrath     *                          1: 1          Call Subroutine 1
;{CR23X}                       *
;Date:9/30/02                  *                        ;Read RTDOhms Measurement
;CR23X Data logger             *                         11:  Full Bridge w/mv Excit (P9)
;*******************************                          1: 1          Reps
*Table 1 Program                                         2: 24         1000 mV, 60 Hz Reject, Slow, Ex Range
  01: 30          Execution Interval (seconds)           3: 24         1000 mV, 60 Hz Reject, Slow, Br Range
                                                         4: 9          DIFF Channel
;If time is 5:00 AM then turn the cell phone on          5: 2          Excite all reps w/Exchan 2
1:  If time is (P92)                                     6: 1000       mV Excitation
  1: 300       Minutes (Seconds --) into a              7: 19         Loc [ RTDOhms    ]
  2: 1440      Interval (same units as above)           8: 259.75     Mult
  3: 41        Set Port 1 High                           9: 0.0        Offset

;If time is 5:00 AM then Set Flag 1 high for battery    ;Read Chemi-resistor mVolt readings
check function                                           12:  Excite-Delay (SE) (P4)
2:  If time is (P92)                                      1: 4          Reps
  1: 300       Minutes (Seconds --) into a              2: 15         5000 mV, Fast Range
  2: 1440      Interval (same units as above)           3: 9          SE Channel
  3: 11        Set Flag 1 High                           4: 1          Excite all reps w/Exchan 1
                                                         5: 0          Delay (0.01 sec units)
;If time is 8:00 PM then turn cell phone off             6: 1          mV Excitation
3:  If time is (P92)                                     7: 1          Loc [ Sen_1_mVm ]
  1: 1200      Minutes (Seconds --) into a              8: -1         Mult
  2: 1440      Interval (same units as above)           9: 0          Offset
  3: 51        Set Port 1 Low
                                                        ;Calculate Ohms from voltage readings
;If time is 8:00 PM then Set Flag 1 low for battery     13:  Z=X+F (P34)
check function                                           1: 1          X Loc [ Sen_1_mVm ]
4:  If time is (P92)                                     2: 5000       F
  1: 1200      Minutes (Seconds --) into a              3: 5          Z Loc [ Res_1_mVc ]
  2: 1440      Interval (same units as above)
  3: 21        Set Flag 1 Low                            14:  Z=X+F (P34)
                                                         1: 2          X Loc [ Sen_2_mVm ]
;Check for battery check flag 1 to be high and if so     2: 5000       F
then                                                     3: 6          Z Loc [ Res_2_mVc ]
5:  If Flag/Port (P91)
  1: 11        Do if Flag 1 is High                      15:  Z=X+F (P34)
  2: 30        Then Do                                   1: 3          X Loc [ Sen_3_mVm ]
                                                         2: 5000       F
     ;If battery voltage is below 11.5 volts then turn   3: 7          Z Loc [ Res_3_mVc ]
cell phone off
    6:  If (X<=>F) (P89)                                 16:  Z=X+F (P34)
      1: 29       X Loc [ Bat_Vdc   ]                    1: 4          X Loc [ Sen_4_mVm ]
      2: 4        <                                      2: 5000       F
      3: 11.5     F                                      3: 8          Z Loc [ Res_4_mVc ]
      4: 51       Set Port 1 Low
                                                         17:  Z=X/Y (P38)
     ;If Battery voltage is above 12.2 volts then turn   1: 5          X Loc [ Res_1_mVc ]
cell phone on                                            2: 20         Y Loc [ Ref1_ohm  ]
    7:  If (X<=>F) (P89)                                 3: 10         Z Loc [ uA_1c     ]
      1: 29       X Loc [ Bat_Vdc   ]
      2: 3        >=                                      18:  Z=X/Y (P38)
      3: 12.2     F                                      1: 6          X Loc [ Res_2_mVc ]
      4: 41       Set Port 1 High                        2: 21         Y Loc [ Ref2_ohm  ]
                                                         3: 11         Z Loc [ uA_2c     ]
8:  End (P95)
                                                         19:  Z=X/Y (P38)
;If time is 0 minutes into a 60 second interval then do  1: 7          X Loc [ Res_3_mVc ]
9:  If time is (P92)                                     2: 22         Y Loc [ Ref3_ohm  ]
  1: 0         Minutes (Seconds --) into a              3: 12         Z Loc [ uA_3c     ]
  2: 60        Interval (same units as above)
  3: 30        Then Do
```

```
20:  Z=X/Y (P38)
 1: 8          X Loc [ Res_4_mVc ]
 2: 23         Y Loc [ Ref4_ohm  ]
 3: 13         Z Loc [ uA_4c     ]

21:  Z=X/Y (P38)
 1: 9          X Loc [ Res_5_mVc ]
 2: 24         Y Loc [ Ref5_ohm  ]
 3: 14         Z Loc [ uA_5c     ]

22:  Z=X/Y (P38)
 1: 1          X Loc [ Sen_1_mVm ]
 2: 10         Y Loc [ uA_1c     ]
 3: 25         Z Loc [ negohms1  ]

23:  Z=X/Y (P38)
 1: 2          X Loc [ Sen_2_mVm ]
 2: 11         Y Loc [ uA_2c     ]
 3: 26         Z Loc [ negohms2  ]

24:  Z=X/Y (P38)
 1: 3          X Loc [ Sen_3_mVm ]
 2: 12         Y Loc [ uA_3c     ]
 3: 27         Z Loc [ negohms3  ]

25:  Z=X/Y (P38)
 1: 4          X Loc [ Sen_4_mVm ]
 2: 13         Y Loc [ uA_4c     ]
 3: 28         Z Loc [ negohms4  ]

26:  Z=X*F (P37)
 1: 25         X Loc [ negohms1  ]
 2: -1         F
 3: 15         Z Loc [ ohms_1c   ]

27:  Z=X*F (P37)
 1: 26         X Loc [ negohms2  ]
 2: -1         F
 3: 15         Z Loc [ ohms_1c   ]

28:  Z=X*F (P37)
 1: 27         X Loc [ negohms3  ]
 2: -1         F
 3: 17         Z Loc [ ohms_3c   ]

29:  Z=X*F (P37)
 1: 28         X Loc [ negohms4  ]
 2: -1         F
 3: 18         Z Loc [ ohms_4c   ]

;Set output flag high
30:  Do (P86)
 1: 10         Set Output Flag High (Flag 0)

;Set Resolution High
31:  Resolution (P78)
 1: 1          High Resolution

;Set time and date option to format needed
32:  Real Time (P77)^1739
 1: 1111       Year,Day,Hour/Minute,Seconds
(midnight = 0000)

;Write to final storage
33:  Sample (P70)^13083
 1: 5          Reps
 2: 15         Loc [ ohms_1c   ]

34:  Sample (P70)^24566
 1: 5          Reps
 2: 40         Loc [ Bat_VdcAv ]

35:  End (P95)

;If time is 0 into a 30 second interval then update
environmental and hardware values
36:  If time is (P92)
 1: 0      -- Minutes (Seconds --) into a
 2: 30     -- Interval (same units as above)
 3: 30         Then Do
```

```
;Update Battery voltage value
37:  Batt Voltage (P10)
 1: 29         Loc [ Bat_Vdc   ]

;Update Panel Temperature
38:  Panel Temperature (P17)
 1: 30         Loc [ Temp_C    ]

;Update RH Temperature
39:  Volt (SE) (P1)
 1: 1          Reps
 2: 24         1000 mV, 60 Hz Reject, Slow Range
 3: 14         SE Channel
 4: 31         Loc [ RHpct     ]
 5: .1         Mult
 6: 0          Offset

;Update RH Temperature value
40:  Volt (SE) (P1)
 1: 1          Reps
 2: 24         1000 mV, 60 Hz Reject, Slow Range
 3: 15         SE Channel
 4: 32         Loc [ RH_Temp_C ]
 5: .1         Mult
 6: -40        Offset

;Update Pressure value
41:  Volt (SE) (P1)
 1: 1          Reps
 2: 15         5000 mV, Fast Range
 3: 23         SE Channel
 4: 33         Loc [ BP_mbar   ]
 5: .184       Mult
 6: 600        Offset

;4.5 minute running average of environmental and
hardware values
42:  Running Average (P52)
 1: 5          Reps
 2: 29         First Source Loc [ Bat_Vdc   ]
 3: 40         First Destination Loc [ Bat_VdcAv ]
 4: 9          Number of Values in Avg Window

43:  End (P95)

*Table 2 Program
 01: .4         Execution Interval (seconds)

;If time is 59 minutes into a 60 minute interval
1:  If time is (P92)
 1: 59         Minutes (Seconds --) into a
 2: 60         Interval (same units as above)
 3: 30         Then Do

    ;Begin loop for 60 seconds
    2:  Beginning of Loop (P87)
     1: 1          Delay
     2: 150        Loop Count

        ;Take SAW voltage measurement
        3:  Volt (Diff) (P2)
         1: 3          Reps
         2: 14         1000 mV, Fast Range
         3: 1          DIFF Channel
         4: 34         Loc [ PVTD1     ]
         5: 1.0        Mult
         6: 0.0        Offset

        ;Running average of SAW measurement
        4:  Running Average (P52)
         1: 3          Reps
         2: 34         First Source Loc [ PVTD1     ]
         3: 37         First Destination Loc [ PVTD1avg
]
         4: 100        Number of Values in Avg Window

    5:  End (P95)

6:  End (P95)

;If time is 0 minutes into a 60 minute interval then do
```

```
7:  If time is (P92)
 1: 0          Minutes (Seconds --) into a
 2: 60         Interval (same units as above)
 3: 10         Set Output Flag High (Flag 0)

;Set resolution High
8:  Resolution (P78)
 1: 1          High Resolution

;Set time and date option to format needed
9:  Real Time (P77)^10737
 1: 1111       Year,Day,Hour/Minute,Seconds (midnight =
0000)

;Write to final storage
10:  Sample (P70)^4868
 1: 3          Reps
 2: 37         Loc [ PVTD1avg ]

11:  Sample (P70)^5767
 1: 3          Reps
 2: 42         Loc [ RHpctAv   ]

*Table 3 Subroutines

;Reference Resistor values
1:  Beginning of Subroutine (P85)
 1: 1          Subroutine 1

2:  Z=F (P30)
 1: 1612.8     F
 2: 0          Exponent of 10
 3: 20         Z Loc [ Ref1_ohm  ]

3:  Z=F (P30)
 1: 1494.3     F
 2: 0          Exponent of 10
 3: 21         Z Loc [ Ref2_ohm  ]

4:  Z=F (P30)
 1: 1323.3     F
 2: 0          Exponent of 10
 3: 22         Z Loc [ Ref3_ohm  ]

5:  Z=F (P30)
 1: 1326.5     F
 2: 0          Exponent of 10
 3: 23         Z Loc [ Ref4_ohm  ]

6:  End (P95)

End Program

-Input Locations-
1 Sen_1_mVm 5 2 1
2 Sen_2_mVm 9 2 1
3 Sen_3_mVm 9 2 1
4 Sen_4_mVm 17 2 1
5 Res_1_mVc 1 1 1
6 Res_2_mVc 1 1 1
7 Res_3_mVc 1 1 1
8 Res_4_mVc 1 1 1
9 Res_5_mVc 1 1 0
10 uA_1c     1 1 1
11 uA_2c     1 1 1
12 uA_3c     1 1 1
13 uA_4c     1 1 1
14 uA_5c     1 0 1
15 ohms_1c   1 1 2
16 ohms_2c   1 1 0
17 ohms_3c   1 1 1
18 ohms_4c   1 1 1
19 RTDOhms   1 1 1
20 Ref1_ohm  1 1 1
21 Ref2_ohm  1 1 1
22 Ref3_ohm  1 1 1
23 Ref4_ohm  1 1 1
24 Ref5_ohm  1 1 0
25 negohms1  1 1 1
26 negohms2  1 1 1
27 negohms3  1 1 1
28 negohms4  1 1 1
29 Bat_Vdc   1 3 1
30 Temp_C    1 1 1
31 RHpct     5 1 1
32 RH_Temp_C 1 1 1
33 BP_mbar   1 1 1
34 PVTD1     5 1 1
35 PVTD2     9 1 1
36 PIB       17 1 1
37 PVTD1avg  5 1 1
38 PVTD2avg  9 1 1
39 PIBavg    17 1 1
40 Bat_VdcAv 5 1 1
41 Temp_CAv  9 1 1
42 RHpctAv   9 2 1
43 RHTempCAv 9 2 1
44 BP_mbarAv 17 2 1
45 _____ 1 0 0
-Program Security-
0000
0000
0000
-Mode 4-
-Final Storage Area 2-
0
-CR10X ID-
0
-CR10X Power Up-
3
-CR10X Compile Setting-
3
-CR10X RS-232 Setting-
-1
-DLD File Labels-
0
-Final Storage Labels-
0,Year_RTM,10737
0,Day_RTM
0,Hour_Minute_RTM
0,Seconds_RTM
1,PVTD1avg~37,4868
1,PVTD2avg~38
1,PIBavg~39
2,RHpctAv~42,5767
2,RHTempCAv~43
2,BP_mbarAv~44
3,Year_RTM,1739
3,Day_RTM
3,Hour_Minute_RTM
3,Seconds_RTM
4,ohms_1c~15,13083
4,ohms_2c~16
4,ohms_3c~17
4,ohms_4c~18
4,RTDOhms~19
5,Bat_VdcAv~40,24566
5,Temp_CAv~41
5,RHpctAv~42
5,RHTempCAv~43
5,BP_mbarAv~44
```

Appendix B.3: Campbell CR23X Data-Logging Program for Chemiresistor and SAW Measurement (Post Test Program, Test Date: 10/23/02-12/9/02)

```
;{CR23X}
;NTS Test Program              *
;Written By: Jerome Wright &   *
;           Lucas McGrath      *
;{CR23X}                        *
;Date:9/30/02                   *
;CR23X Data logger              *
;********************************
*Table 1 Program
  01: 30          Execution Interval (seconds)

;If time is 5:00 AM then turn the cell phone on
1:  If time is (P92)
  1: 300      Minutes (Seconds --) into a
  2: 1440     Interval (same units as above)
  3: 41       Set Port 1 High

;If time is 5:00 then Set Flag 1 high for battery check
function
2:  If time is (P92)
  1: 300      Minutes (Seconds --) into a
  2: 1440     Interval (same units as above)
  3: 11       Set Flag 1 High

;If time is 8:00 PM then turn cell phone off
3:  If time is (P92)
  1: 1200     Minutes (Seconds --) into a
  2: 1440     Interval (same units as above)
  3: 51       Set Port 1 Low

;If time is 8:00 PM then Set Flag 1 low for battery
check function
4:  If time is (P92)
  1: 1200     Minutes (Seconds --) into a
  2: 1440     Interval (same units as above)
  3: 21       Set Flag 1 Low

;Check for battery check flag 1 to be high and if so
then do
5:  If Flag/Port (P91)
  1: 11       Do if Flag 1 is High
  2: 30       Then Do

    ;If battery voltage is below 11.5 volts then turn
cell phone off
    6:  If (X<=>F) (P89)
      1: 29       X Loc [ Bat_Vdc  ]
      2: 4        <
      3: 11.5     F
      4: 51       Set Port 1 Low

    ; If battery voltage is above 12.2 volts then turn
cell phone on
    7:  If (X<=>F) (P89)
      1: 29       X Loc [ Bat_Vdc  ]
      2: 3        >=
      3: 12.2     F
      4: 41       Set Port 1 High

8:  End (P95)

;If the time is 0 minutes into a 60 second interval
then do
9:  If time is (P92)
  1: 0        Minutes (Seconds --) into a
  2: 60       Interval (same units as above)
  3: 30       Then Do

    ;Calls subroutine to load values in the subroutine
    10: Do (P86)
      1: 1        Call Subroutine 1

    ;Read RTDOhms Measurement
    11: Full Bridge w/mv Excit (P9)
      1: 1        Reps
```

```
      2: 24       1000 mV, 60 Hz Reject, Slow, Ex Range
      3: 24       1000 mV, 60 Hz Reject, Slow, Br Range
      4: 9        DIFF Channel
      5: 2        Excite all reps w/Exchan 2
      6: 1000     mV Excitation
      7: 19       Loc [ RTDOhms   ]
      8: 259.75   Mult
      9: 0.0      Offset

;Read Chemi-resistor mVolt readings
12:  Excite-Delay (SE) (P4)
  1: 4        Reps
  2: 15       5000 mV, Fast Range
  3: 9        SE Channel
  4: 1        Excite all reps w/Exchan 1
  5: 0        Delay (0.01 sec units)
  6: 5000     mV Excitation
  7: 1        Loc [ Sen_1_mVm ]
  8: -1       Mult
  9: 0        Offset

;Calculate Ohms from Voltage reading
13:  Z=X+F (P34)
  1: 1        X Loc [ Sen_1_mVm ]
  2: 5000     F
  3: 5        Z Loc [ Res_1_mVc ]

14:  Z=X+F (P34)
  1: 2        X Loc [ Sen_2_mVm ]
  2: 5000     F
  3: 6        Z Loc [ Res_2_mVc ]

15:  Z=X+F (P34)
  1: 3        X Loc [ Sen_3_mVm ]
  2: 5000     F
  3: 7        Z Loc [ Res_3_mVc ]

16:  Z=X+F (P34)
  1: 4        X Loc [ Sen_4_mVm ]
  2: 5000     F
  3: 8        Z Loc [ Res_4_mVc ]

17:  Z=X/Y (P38)
  1: 5        X Loc [ Res_1_mVc ]
  2: 20       Y Loc [ Ref1_ohm  ]
  3: 10       Z Loc [ uA_1c     ]

18:  Z=X/Y (P38)
  1: 6        X Loc [ Res_2_mVc ]
  2: 21       Y Loc [ Ref2_ohm  ]
  3: 11       Z Loc [ uA_2c     ]

19:  Z=X/Y (P38)
  1: 7        X Loc [ Res_3_mVc ]
  2: 22       Y Loc [ Ref3_ohm  ]
  3: 12       Z Loc [ uA_3c     ]

20:  Z=X/Y (P38)
  1: 8        X Loc [ Res_4_mVc ]
  2: 23       Y Loc [ Ref4_ohm  ]
  3: 13       Z Loc [ uA_4c     ]

21:  Z=X/Y (P38)
  1: 9        X Loc [ Res_5_mVc ]
  2: 24       Y Loc [ Ref5_ohm  ]
  3: 14       Z Loc [ uA_5c     ]

22:  Z=X/Y (P38)
  1: 1        X Loc [ Sen_1_mVm ]
  2: 10       Y Loc [ uA_1c     ]
  3: 25       Z Loc [ negohms1  ]

23:  Z=X/Y (P38)
  1: 2        X Loc [ Sen_2_mVm ]
  2: 11       Y Loc [ uA_2c     ]
```

```
     3: 26        Z Loc [ negohms2  ]

  24:  Z=X/Y (P38)
     1: 3         X Loc [ Sen_3_mVm ]
     2: 12        Y Loc [ uA_3c     ]
     3: 27        Z Loc [ negohms3  ]

  25:  Z=X/Y (P38)
     1: 4         X Loc [ Sen_4_mVm ]
     2: 13        Y Loc [ uA_4c     ]
     3: 28        Z Loc [ negohms4  ]

  26:  Z=X*F (P37)
     1: 25        X Loc [ negohms1  ]
     2: -1        F
     3: 15        Z Loc [ ohms_1c   ]

  27:  Z=X*F (P37)
     1: 26        X Loc [ negohms2  ]
     2: -1        F
     3: 16        Z Loc [ ohms_2c   ]

  28:  Z=X*F (P37)
     1: 27        X Loc [ negohms3  ]
     2: -1        F
     3: 17        Z Loc [ ohms_3c   ]

  29:  Z=X*F (P37)
     1: 28        X Loc [ negohms4  ]
     2: -1        F
     3: 18        Z Loc [ ohms_4c   ]

  ;Temp Diff
  30:  Z=X+F (P34)
     1: 32        X Loc [ RH_Temp_C ]
     2: -23       F
     3: 45        Z Loc [ TempDiff  ]

  ;Temperature Correction Value
  31:  Z=X*Y (P36)
     1: 45        X Loc [ TempDiff  ]
     2: 46        Y Loc [ TempSlo1  ]
     3: 50        Z Loc [ TempCor1  ]

  32:  Z=X*Y (P36)
     1: 45        X Loc [ TempDiff  ]
     2: 47        Y Loc [ TempSlo2  ]
     3: 51        Z Loc [ TempCor2  ]

  33:  Z=X*Y (P36)
     1: 45        X Loc [ TempDiff  ]
     2: 48        Y Loc [ TempSlo3  ]
     3: 52        Z Loc [ TempCor3  ]

  34:  Z=X*Y (P36)
     1: 45        X Loc [ TempDiff  ]
     2: 49        Y Loc [ TempSlo4  ]
     3: 53        Z Loc [ TempCor4  ]

  ;Subtract the Temperature correction value from
  Actual Resistance
  35:  Z=X-Y (P35)
     1: 15        X Loc [ ohms_1c   ]
     2: 50        Y Loc [ TempCor1  ]
     3: 54        Z Loc [ TempCorR1 ]

  36:  Z=X-Y (P35)
     1: 16        X Loc [ ohms_2c   ]
     2: 51        Y Loc [ TempCor2  ]
     3: 55        Z Loc [ TempCorR2 ]

  37:  Z=X-Y (P35)
     1: 17        X Loc [ ohms_3c   ]
     2: 52        Y Loc [ TempCor3  ]
     3: 56        Z Loc [ TempCorR3 ]

  38:  Z=X-Y (P35)
     1: 18        X Loc [ ohms_4c   ]
     2: 53        Y Loc [ TempCor4  ]
     3: 57        Z Loc [ TempCorR4 ]

  ;Subtract Baseline Value from Temperature
  corrected value
  39:  Z=X-Y (P35)
     1: 54        X Loc [ TempCorR1 ]
     2: 58        Y Loc [ BaseLine1 ]
     3: 62        Z Loc [ Num1      ]

  40:  Z=X-Y (P35)
     1: 55        X Loc [ TempCorR2 ]
     2: 59        Y Loc [ BaseLine2 ]
     3: 63        Z Loc [ Num2      ]

  41:  Z=X-Y (P35)
     1: 56        X Loc [ TempCorR3 ]
     2: 60        Y Loc [ BaseLine3 ]
     3: 64        Z Loc [ Num3      ]

  42:  Z=X-Y (P35)
     1: 57        X Loc [ TempCorR4 ]
     2: 61        Y Loc [ BaseLine4 ]
     3: 65        Z Loc [ Num4      ]

  ;Divide Numerator by the baseline
  43:  Z=X/Y (P38)
     1: 62        X Loc [ Num1      ]
     2: 58        Y Loc [ BaseLine1 ]
     3: 66        Z Loc [ DeltaRB1_ ]

  44:  Z=X/Y (P38)
     1: 63        X Loc [ Num2      ]
     2: 59        Y Loc [ BaseLine2 ]
     3: 67        Z Loc [ DeltaRB2  ]

  45:  Z=X/Y (P38)
     1: 64        X Loc [ Num3      ]
     2: 60        Y Loc [ BaseLine3 ]
     3: 68        Z Loc [ DeltaRB3  ]

  46:  Z=X/Y (P38)
     1: 65        X Loc [ Num4      ]
     2: 61        Y Loc [ BaseLine4 ]
     3: 69        Z Loc [ DeltaRB4  ]

  ;Delta R/Rb To the Power of ExCon() for power
  curve fit
  47:  Z=X^Y (P47)
     1: 66        X Loc [ DeltaRB1_ ]
     2: 70        Y Loc [ ExCon1    ]
     3: 78        Z Loc [ DeltaX1   ]

  48:  Z=X^Y (P47)
     1: 67        X Loc [ DeltaRB2  ]
     2: 71        Y Loc [ ExCon2    ]
     3: 79        Z Loc [ DeltaX2   ]

  49:  Z=X^Y (P47)
     1: 68        X Loc [ DeltaRB3  ]
     2: 72        Y Loc [ ExCon3    ]
     3: 80        Z Loc [ DeltaX3   ]

  50:  Z=X^Y (P47)
     1: 69        X Loc [ DeltaRB4  ]
     2: 73        Y Loc [ ExCon4    ]
     3: 81        Z Loc [ DeltaX4   ]

  ;Multiply by Coefficient for power-law fit
  51:  Z=X*Y (P36)
     1: 78        X Loc [ DeltaX1   ]
     2: 74        Y Loc [ Coef1     ]
     3: 82        Z Loc [ PECH_Con  ]

  52:  Z=X*Y (P36)
     1: 79        X Loc [ DeltaX2   ]
     2: 75        Y Loc [ Coef2     ]
     3: 83        Z Loc [ PNVP_Con  ]

  53:  Z=X*Y (P36)
     1: 80        X Loc [ DeltaX3   ]
     2: 76        Y Loc [ Coef3     ]
     3: 84        Z Loc [ PIB_Con   ]
```

```
    54:  Z=X*Y (P36)                              3: 40        First Destination Loc [ Bat_VdcAv ]
     1: 81        X Loc [ DeltaX4   ]             4: 9         Number of Values in Avg Window
     2: 77        Y Loc [ Coef4     ]
     3: 85        Z Loc [ PEVA_Con  ]       69:  End (P95)

    ;Set Output Flag High
    55:  Do (P86)                           *Table 2 Program
     1: 10        Set Output Flag High (Flag 0)    01:  .4         Execution Interval (seconds)

    ;Set Resolution High                    ;If time is 59 minutes into a 60 minute interval then
    56:  Resolution (P78)                   do
     1: 1         High Resolution           1:  If time is (P92)
                                             1: 59       Minutes (Seconds --) into a
    ;Set Time and date option to format needed      2: 60       Interval (same units as above)
    57:  Real Time (P77)^28398               3: 30       Then Do
     1: 1111      Year,Day,Hour/Minute,Seconds
(midnight = 0000)                               ;Begin loop for 60 seconds
                                                2:  Beginning of Loop (P87)
    ;Write to final storage                      1: 1         Delay
    58:  Sample (P70)^12425                      2: 150       Loop Count
     1: 5         Reps
     2: 15        Loc [ ohms_1c    ]              ;Take SAW voltage measurement
                                                 3:  Volt (Diff) (P2)
    59:  Sample (P70)^4246                        1: 3         Reps
     1: 5         Reps                            2: 14        1000 mV, Fast Range
     2: 40        Loc [ Bat_VdcAv ]               3: 1         DIFF Channel
                                                  4: 34        Loc [ PVTD1     ]
    60:  Sample (P70)^15654                       5: 1.0       Mult
     1: 4         Reps                            6: 0.0       Offset
     2: 82        Loc [ PECH_Con   ]
                                                 ;Running average of SAW measurements
61:  End (P95)                                   4:  Running Average (P52)
                                                  1: 3         Reps
;If time is 0 into a 30 second interval then update       2: 34        First Source Loc [ PVTD1     ]
environmental and hardware values                3: 37        First Destination Loc [ PVTD1avg
62:  If time is (P92)                       ]
 1: 0    -- Minutes (Seconds --) into a          4: 100       Number of Values in Avg Window
 2: 30   -- Interval (same units as above)
 3: 30        Then Do                          5:  End (P95)

    ;Update Battery voltage value           6:  End (P95)
    63:  Batt Voltage (P10)
     1: 29        Loc [ Bat_Vdc   ]          ;If time is 0 minutes into a 60 minute interval then do
                                             7:  If time is (P92)
    ;Update Panel Temperature value          1: 0         Minutes (Seconds --) into a
    64:  Panel Temperature (P17)             2: 60        Interval (same units as above)
     1: 30        Loc [ Temp_C    ]          3: 10        Set Output Flag High (Flag 0)

    ;Update RH value                        ;Set Resolution High
    65:  Volt (SE) (P1)                     8:  Resolution (P78)
     1: 1         Reps                        1: 1         High Resolution
     2: 24        1000 mV, 60 Hz Reject, Slow Range
     3: 14        SE Channel                ;Set Time and date option to format needed
     4: 31        Loc [ RHpct     ]         9:  Real Time (P77)
     5: .1        Mult                        1: 1111      Year,Day,Hour/Minute,Seconds (midnight =
     6: 0         Offset                     0000)

    ;Update RH Temperature value            ;Write to final storage
    66:  Volt (SE) (P1)                     10:  Sample (P70)
     1: 1         Reps                        1: 3         Reps
     2: 24        1000 mV, 60 Hz Reject, Slow Range       2: 37        Loc [ PVTD1avg  ]
     3: 15        SE Channel
     4: 32        Loc [ RH_Temp_C ]         11:  Sample (P70)
     5: .1        Mult                        1: 3         Reps
     6: -40       Offset                      2: 42        Loc [ RHpctAv   ]

    ;Update Pressure value
    67:  Volt (SE) (P1)
     1: 1         Reps                       *Table 3 Subroutines
     2: 15        5000 mV, Fast Range
     3: 23        SE Channel                1:  Beginning of Subroutine (P85)
     4: 33        Loc [ BP_mbar   ]          1: 1         Subroutine 1
     5: .184      Mult
     6: 600       Offset                    ;Reference resistor values
                                            2:  Z=F (P30)
    ;4.5 minute running average of environmental and        1: 1612.8    F
hardware values                             2: 0         Exponent of 10
    68:  Running Average (P52)               3: 20        Z Loc [ Ref1_ohm ]
     1: 5         Reps
     2: 29        First Source Loc [ Bat_Vdc   ]      3:  Z=F (P30)
                                             1: 1494.3    F
```

```
    2:  0        Exponent of 10                  2:  00       Exponent of 10
    3:  21       Z Loc [ Ref2_ohm  ]             3:  74       Z Loc [ Coef1     ]

    4:  Z=F (P30)                            19:   Z=F (P30)
    1:  1323.3   F                               1:  2.042    F
    2:  0        Exponent of 10                  2:  00       Exponent of 10
    3:  22       Z Loc [ Ref3_ohm  ]             3:  75       Z Loc [ Coef2     ]

    5:  Z=F (P30)                            20:   Z=F (P30)
    1:  1326.5   F                               1:  .5608    F
    2:  0        Exponent of 10                  2:  00       Exponent of 10
    3:  23       Z Loc [ Ref4_ohm  ]             3:  76       Z Loc [ Coef3     ]

;Input Slope Values for Temperature Correction (PECH,     21:   Z=F (P30)
PNVP, PIB, PEVA)                                             1:  .1275    F
    6:  Z=F (P30)                                2:  00       Exponent of 10
    1:  .4199    F                               3:  77       Z Loc [ Coef4     ]
    2:  00       Exponent of 10
    3:  46       Z Loc [ TempSlo1 ]

    7:  Z=F (P30)
    1:  .6049    F
    2:  00       Exponent of 10
    3:  47       Z Loc [ TempSlo2  ]

    8:  Z=F (P30)                            22:   End (P95)
    1:  .9346    F
    2:  00       Exponent of 10             End Program
    3:  48       Z Loc [ TempSlo3  ]
                                            -Input Locations-
    9:  Z=F (P30)                            1 Sen_1_mVm 5 2 1
    1:  4.556    F                           2 Sen_2_mVm 9 2 1
    2:  00       Exponent of 10              3 Sen_3_mVm 9 2 1
    3:  49       Z Loc [ TempSlo4  ]         4 Sen_4_mVm 17 2 1
                                             5 Res_1_mVc 1 1 1
;Baseline Values                            6 Res_2_mVc 1 1 1
   10:  Z=F (P30)                            7 Res_3_mVc 1 1 1
    1:  301.69   F                           8 Res_4_mVc 1 1 1
    2:  00       Exponent of 10              9 Res_5_mVc 1 1 0
    3:  58       Z Loc [ BaseLine1 ]        10 uA_1c      1 1 1
                                           11 uA_2c      1 1 1
   11:  Z=F (P30)                           12 uA_3c      1 1 1
    1:  260.55   F                          13 uA_4c      1 1 1
    2:  00       Exponent of 10             14 uA_5c      1 0 1
    3:  59       Z Loc [ BaseLine2 ]        15 ohms_1c    1 2 1
                                           16 ohms_2c    1 2 1
   12:  Z=F (P30)                           17 ohms_3c    1 2 1
    1:  480.23   F                          18 ohms_4c    1 2 1
    2:  00       Exponent of 10             19 RTDOhms    1 1 1
    3:  60       Z Loc [ BaseLine3 ]        20 Ref1_ohm   1 1 1
                                           21 Ref2_ohm   1 1 1
   13:  Z=F (P30)                           22 Ref3_ohm   1 1 1
    1:  432.2    F                          23 Ref4_ohm   1 1 1
    2:  00       Exponent of 10             24 Ref5_ohm   1 1 0
    3:  61       Z Loc [ BaseLine4 ]        25 negohms1   1 1 1
                                           26 negohms2   1 1 1
;Exponent for Concentration Conversion     27 negohms3   1 1 1
   14:  Z=F (P30)                           28 negohms4   1 1 1
    1:  .8415    F                          29 Bat_Vdc    1 3 1
    2:  00       Exponent of 10             30 Temp_C     1 1 1
    3:  70       Z Loc [ ExCon1     ]       31 RHpct      1 1 1
                                           32 RH_Temp_C 1 2 1
   15:  Z=F (P30)                           33 BP_mbar    1 1 1
    1:  .8768    F                          34 PVTD1      5 1 1
    2:  00       Exponent of 10             35 PVTD2      9 1 1
    3:  71       Z Loc [ ExCon2     ]       36 PIB       17 1 1
                                           37 PVTD1avg   5 1 1
   16:  Z=F (P30)                           38 PVTD2avg   9 1 1
    1:  .8754    F                          39 PIBavg    17 1 1
    2:  00       Exponent of 10             40 Bat_VdcAv  5 1 1
    3:  72       Z Loc [ ExCon3     ]       41 Temp_CAv   9 1 1
                                           42 RHpctAv    9 2 1
   17:  Z=F (P30)                           43 RHTempCAv 9 2 1
    1:  .6855    F                          44 BP_mbarAv 17 2 1
    2:  00       Exponent of 10             45 TempDiff   1 4 1
    3:  73       Z Loc [ ExCon4     ]       46 TempSlo1   1 1 1
                                           47 TempSlo2   1 1 1
;Coefficient for Concentration Conversion using Power-    48 TempSlo3   1 1 1
Law                                        49 TempSlo4   1 1 1
   18:  Z=F (P30)                           50 TempCor1   1 1 1
    1:  1.579    F                          51 TempCor2   1 1 1
                                           52 TempCor3   1 1 1
                                           53 TempCor4   1 1 1
```

```
54 TempCorR1 1 1 1                          0
55 TempCorR2 1 1 1                          -CR10X Power Up-
56 TempCorR3 1 1 1                          3
57 TempCorR4 1 1 1                          -CR10X Compile Setting-
58 BaseLine1 1 2 1                          3
59 BaseLine2 1 2 1                          -CR10X RS-232 Setting-
60 BaseLine3 1 2 1                          -1
61 BaseLine4 1 2 1                          -DLD File Labels-
62 Num1      1 1 1                          0
63 Num2      1 1 1                          -Final Storage Labels-
64 Num3      1 1 1                          0,Year_RTM,21833
65 Num4      1 1 1                          0,Day_RTM
66 DeltaRB1_ 1 1 1                          0,Hour_Minute_RTM
67 DeltaRB2  1 1 1                          0,Seconds_RTM
68 DeltaRB3  1 1 1                          1,PVTD1avg~37,3393
69 DeltaRB4  1 1 1                          1,PVTD2avg~38
70 ExCon1    1 1 1                          1,PIBavg~39
71 ExCon2    1 1 1                          2,RHpctAv~42,20987
72 ExCon3    1 1 1                          2,RHTempCAv~43
73 ExCon4    1 1 1                          2,BP_mbarAv~44
74 Coef1     1 1 1                          3,Year_RTM,28398
75 Coef2     1 1 1                          3,Day_RTM
76 Coef3     1 1 1                          3,Hour_Minute_RTM
77 Coef4     1 1 1                          3,Seconds_RTM
78 DeltaX1   1 1 1                          4,ohms_1c~15,12425
79 DeltaX2   1 1 1                          4,ohms_2c~16
80 DeltaX3   1 1 1                          4,ohms_3c~17
81 DeltaX4   1 1 1                          4,ohms_4c~18
82 PECH_Con  1 1 1                          4,RTDOhms~19
83 PNVP_Con  1 1 1                          5,Bat_VdcAv~40,4246
84 PIB_Con   1 1 1                          5,Temp_CAv~41
85 PEVA_Con  1 1 1                          5,RHpctAv~42
-Program Security-                          5,RHTempCAv~43
0000                                        5,BP_mbarAv~44
0000                                        6,PECH_Con~82,15654
0000                                        6,PNVP_Con~83
-Mode 4-                                    6,PIB_Con~84
-Final Storage Area 2-                      6,PEVA_Con~85
0
-CR10X ID-
```

Appendix B.4: Campbell CR23X Data-Logging Sample Output for Chemiresistor and SAW Measurement (Post Test Program)

```
130,2002,283,1030,.1,302.08,265.21,492.25,559.35,232.89,11.738,20.391,21.855,21.677,913.37
207,2002,283,1030,.2,140.33,236.23,-860.9,21.847,21.677,913.36
130,2002,283,1035,.1,302.08,265.21,492.24,559.16,232.89,12.403,20.516,21.826,21.687,913.32
207,2002,283,1035,.2,140.28,235.93,-860.08,21.831,21.688,913.32
130,2002,283,1040,.1,302.07,265.2,492.07,558.97,232.89,12.599,20.574,21.856,21.69,913.29
207,2002,283,1040,.2,140.18,236.18,-859.92,21.855,21.687,913.28
130,2002,283,1045,.1,302.08,265.21,492.08,558.98,232.91,12.498,20.596,21.824,21.695,913.19
207,2002,283,1045,.2,141.58,235.53,-859.92,21.822,21.696,913.19
130,2002,283,1050,.1,302.07,265.21,492.07,558.98,232.91,12.526,20.579,21.808,21.691,913.17
207,2002,283,1050,.2,141.98,235.19,-859.94,21.809,21.692,913.17
```

Appendix B.5: Campbell CR23X Data-Logging Sample Output for Chemiresistor and SAW Measurement (Post Test Program)

```
155,2002,296,1100,.2,299.84,263.84,485.36,450.33,231.38,12.757,14.391,27.506,19.077,908.75,0,.07108,.01688,.02317
207,2002,296,1100,.3,153.78,257.55,-859.91,27.498,19.08,908.75
155,2002,296,1200,.2,300.05,263.77,485.52,450.49,231.48,12.729,17.656,27.352,19.191,908.09,0,.06968,.01702,.02308
207,2002,296,1200,.3,153.14,258.31,-859.33,27.351,19.189,908.08
155,2002,296,1300,.2,299.97,263.83,485.53,450.51,231.52,12.714,21.071,27.412,19.201,907.17,0,.07011,.01697,.023
207,2002,296,1300,.3,153.54,258.74,-858.34,27.41,19.205,907.16
155,2002,296,1400,.2,300.19,263.9,485.86,450.99,231.64,12.701,24.15,27.004,19.603,906.06,0,.0682,.01692,.02242
207,2002,296,1400,.3,152.2,258.22,-859.51,26.995,19.605,906.06
155,2002,296,1500,.2,300.15,263.86,486.11,451.4,231.75,12.706,25.665,26.848,19.888,905.89,0,.06585,.01688,.022
207,2002,296,1500,.3,151.3,256.92,-860.52,26.832,19.889,905.91
155,2002,296,1600,.2,300.29,263.86,486.11,451.55,231.79,12.722,25.326,26.852,19.977,906.96,0,.06532,.01675,.02192
207,2002,296,1600,.3,151.37,256,-861.46,26.846,19.977,907.02
```

Appendix C: Calibration Curves for Chemiresistor Array C4

The calibration of chemiresistor array C4 was performed by introducing known concentrations of TCE and water vapor to each of the four polymers (from left to right in Figure 2): polyepichlorohydrin (PECH), poly(N-vinyl pyrrolidone) (PNVP), polyisobutylene (PIB), and poly(ethylene-vinyl acetate) copolymer (PEVA). However, the process was slightly different than that described in Section 2.3. Digitally controlled mass-flow controllers were used to maintain precise flow rates of pure nitrogen through bubblers containing liquid TCE and water to the chemiresistor polymers. The tests were conducted at two different chemiresistor temperatures: 22 °C (room temperature (RT)) and 30 °C (in a controlled oven). In addition, the TCE exposures were conducted at two different relative humidities: 0% (pure TCE in nitrogen) and 100% relative humidity (RH) at room temperature. In the latter case, controlled amounts of TCE vapor were passed through the water bubbler until the water reached equilibrium with the flowing TCE vapor. This allowed known concentrations of TCE to be introduced to the chemiresistor polymers under 100% relative humidity conditions. Figure 46 through Figure 49 shows the results of these calibrations.
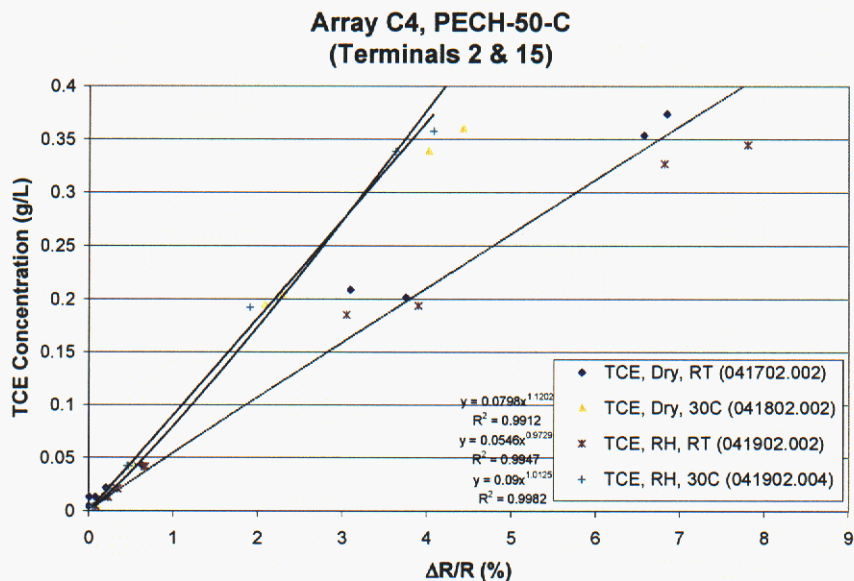

Figure 46. Calibration curves for PECH polymer on chip C4.

Array C4, PNVP-50-C
(Terminals 3 & 15)
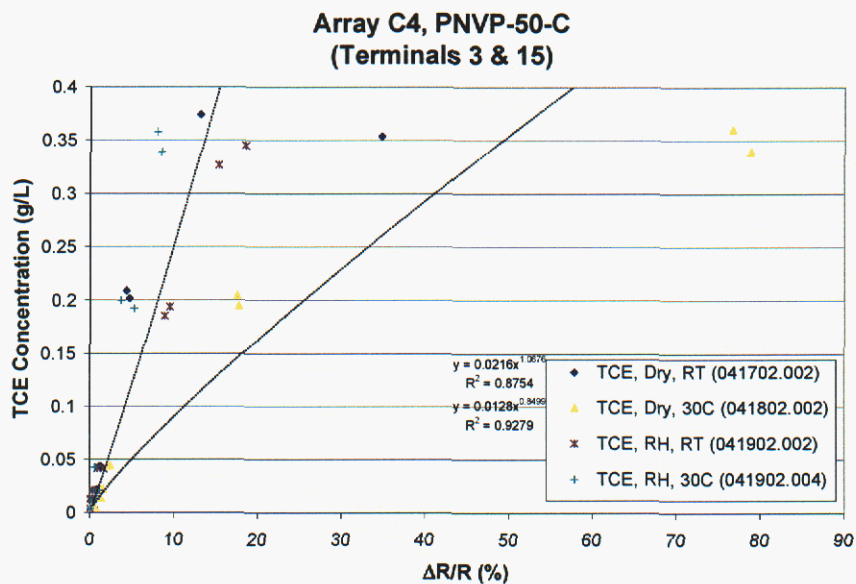
Figure 47. Calibration curves for PNVP polymer on chip C4.

Array C4, PIB-50-C
(Terminals 5 & 13)
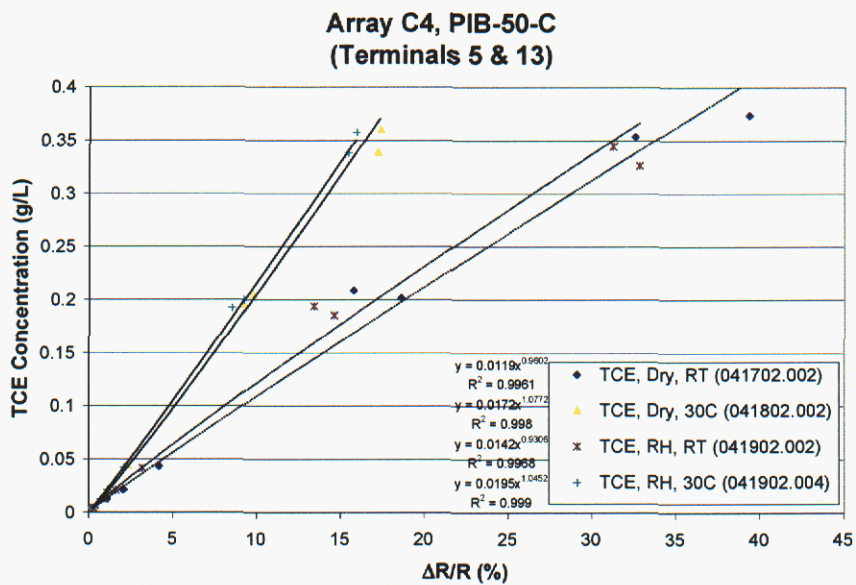
Figure 48. Calibration curves for PIB polymer on chip C4.

Array C4, PEVA-40-C
**(Terminals 7 & 10)**
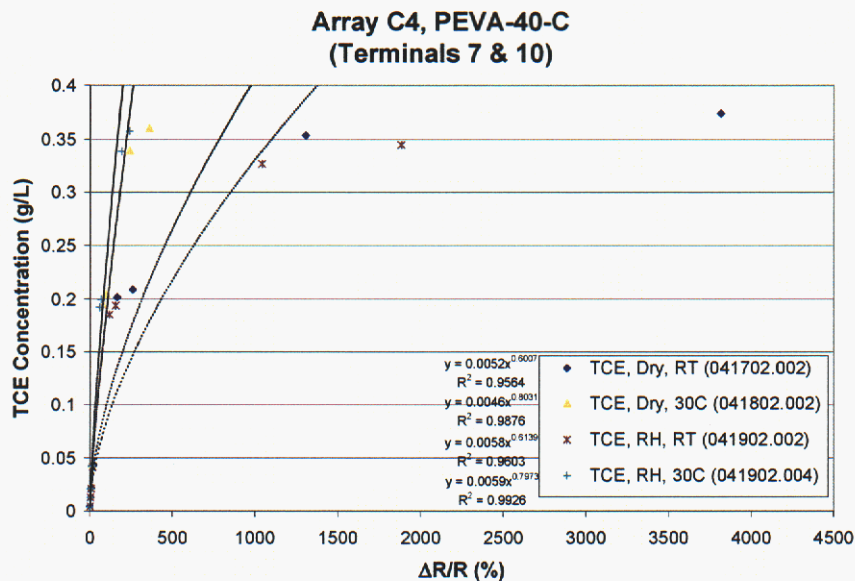
Figure 49. Calibration curves for PEVA polymer on chip C4.

Appendix D: Data-Logger Equations for E2 Chemiresistor

The calibrations and temperature corrections to convert E2 chemiresistor resistances to TCE concentrations (g/L) were programmed directly into the Campbell data logger during the long-term ambient monitoring period (October-December, 2002).

$$PECH\_concentration = 1.579\left[\frac{[R-0.4199(T-23)]-301.69}{301.69}\right]^{0.8415} \quad [g/L]$$

$$PNVP\_concentration = 2.042\left[\frac{[R-0.6049(T-23)]-260.55}{260.55}\right]^{0.8768} \quad [g/L]$$

$$PIB\_concentration = 0.5608\left[\frac{[R-0.9346(T-23)]-480.23}{480.23}\right]^{0.8754} \quad [g/L]$$

$$PEVA\_concentration = 0.1275\left[\frac{[R-4.556(T-23)]-432.2}{432.2}\right]^{0.6855} \quad [g/L]$$

where:

R = Measured Resistance (Ohms) from each of the four chemiresistors
T = Measured Temperature (°C) from the RH/Temperature probe

76

Distribution